SELF-ORGANIZATION AND RESOURCE ALLOCATION IN WIRELESS SENSOR NETWORKS

by

LIANG ZHAO

Presented to the Faculty of the Graduate School of

The University of Texas at Arlington in Partial Fulfillment

of the Requirements

for the Degree of

DOCTOR OF PHILOSOPHY

THE UNIVERSITY OF TEXAS AT ARLINGTON

May 2006

This dissertation is dedicated to my parents, Shuming Zhao and Lili Zhang, for instilling in me the values of hard work, a good attitude and persistence, and for stressing the value of education.

ACKNOWLEDGEMENTS

I would like to thank my supervising professor Dr. Qilian Liang for constantly motivating and encouraging me, and also for his invaluable advice during the course of my doctoral studies. I wish to thank my academic advisors Dr. Jonathan Bredow, Dr. Soontorn Oraintara, Dr. Dan Popa, and Dr. Weidong Zhou for their interest in my research and for taking time to serve on my dissertation committee.

April 12, 2006

ABSTRACT

SELF-ORGANIZATION AND RESOURCE ALLOCATION
IN WIRELESS SENSOR NETWORKS

Publication No. _____

Liang Zhao, Ph.D.

The University of Texas at Arlington, 2006

Supervising Professor: Liang, Qilian

In this dissertation, we utilize clustering to organize wireless sensors into an energy-efficient hierarchy. We propose a Medium-Contention Based ClusterHeadship Auction (MCCHA) scheme, through which sensors self-organize themselves into energy-efficient clusters by bidding for cluster headship. This scheme is based on a new criterion that can be used by each sensor node to make a distributed decision on whether electing to be a cluster head or a non-head member, which is a fully distributed approach. Although MCCHA uses only local information, it achieves better performance in terms of effective lifetime and Data/Energy Ratio compared with native LEACH, which relies on other routing algorithms to access global information. A complementary exponential data correlation model is also introduced to simulate different data aggregation effect.

To better understand the clustering issue in wireless sensor networks, we model the end-to-end distance for a given number of hops in dense planar Wireless Sensor Networks in this dissertation. We derive that the single-hop distance and postulate Beta distribution for 2-hop distance shows Beta distribution for two hops. The multi-hop distance approaches Gaussian when the number of hops is three or greater. Our error analysis also shows the distance error can be minimized by exploiting the distribution knowledge.

Based on this model, we propose a Maximum Likelihood decision to decide to the number of hops given the distance between two nodes. Due to the computational complexity of conditional pdf of the number of hops given the distance, we also propose an attenuated Gaussian approximation for the conditional pdf. We show that the approximation visibly simplifies the decision process and the error analysis. The latency and energy consumption estimation are also included as application examples. Simulations show that our approximation model can predict the latency and energy consumption with less than half RMSE, compared to the linear models.

In this dissertation, we also study the optimal cluster size in Underwater Acoustic networks. Due to the sparse deployment and channel property, the clustering characteristics of UA is different from that of aerial sensor networks. We show that the optimal cluster size is also relevant to the working frequency of the acoustic transmission.

TABLE OF CONTENTS

LIST OF FIGURES

LIST OF TABLES

CHAPTER 1

INTRODUCTION

1.1 Wireless Sensor Networks and Clustering

A wireless sensor network (WSN) can be thought of as an *ad hoc* network consisting of sensors linked by a wireless medium to perform distributed sensing tasks. WSNs share many communication technologies with *ad hoc* networks, but there are some vital differences such as dense deployment and energy constraint [1], thus the protocols developed for traditional wireless ad hoc networks are not necessarily well suited to the unique features of WSNs. When a wireless sensor may have to operate for a relatively long duration on a tiny battery, energy efficiency becomes a major concern [2–5].

A variety of "power-aware" routing protocols have been proposed to address this problem [6–10]. In one school of thoughts [11–16], the traditional Shortest Path First strategy is replaced by Least Energy First routing, i.e., a multi-hop route is preferred to a single-hop one if only multiple short-distance relays cost less energy than a single long-distance transmission. For example, "Minimum Transmission Energy"(MTE) routing [12, 13] was proposed in place of traditional "minimum hops routing". Another school of thoughts is that nodes are clustered so that a hierarchy is formed [17–22]. Based on the observations on cellular networks [23], it would be advisable to partition nodes into clusters for the reasons such as spatial reuse, less update cost, less routing information and less data transmission [24–34]. LEACH (Low-Energy Adaptive Clustering Hierarchy) [35], an example of the latter school, can extend network lifetime by an order of magnitude compared with general-purpose multihop approaches. In conclusion, the characteristics of WSN prefer hierarchical structure with clusterheads [36–38].

However, the cluster formation in LEACH is based on global information. To access such information, other routing schemes are required. In this sense, LEACH is only a

semi-distributed protocol for WSN. Another problem with LEACH is the random head election that cannot guarantee that the desired number of cluster heads be elected or the elected heads evenly positioned. In this paper, we are concerned to optimize the cluster formation using only local information. The intuition behind the proposed Medium-Contention Based ClusterHeadship Auction (MCCHA) is using medium contention to keep the cluster size within an ideal range.

1.2 Localization

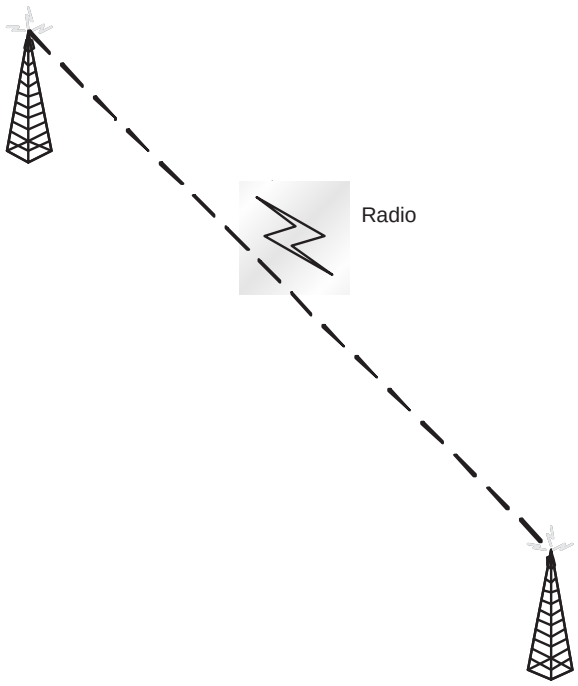

Figure 1.1. ToA ranging.

In Wireless Sensor Networks (WSN), node location information is often required in many applications such as event tracing, environment monitoring and geographic routing [39, 40]. Generally, the distances from a node with unknown location to several anchor nodes are estimated, and then a multilateration is applied to estimate the node location. Distance is often estimated based on received signal strength, time of arrival (TOA), time difference of arrival (TDOA) or angle of arrival [41–43].

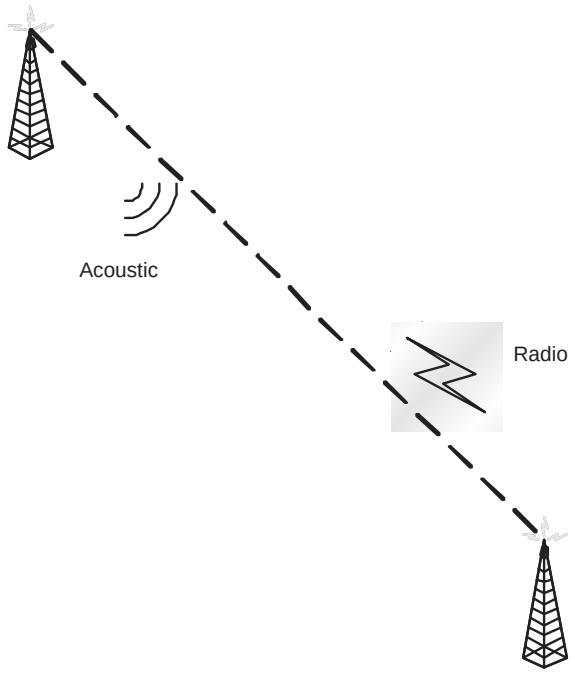

Figure 1.2. TDOA ranging.

The angle-of-arrival based ranging requires directive antennas or arrays, which is not suitable for most microsensors. TOA measures the flight time of radio or acoustic signal and then multiply it by the speed of the signal to estimate the flight distance. The problem with TOA is measuring time of flight requires timing device with satisfactory resolution like in GPS. TDOA uses two different signal with tremendous speed difference so that the flight time can approximated by the difference between arrival time of two signals [44]. Although it needs much less resolution, it often requires extra acoustic or ultrasound emission, which comes with higher price, larger size and more energy consumption, all seeming impractical for microsensors. And all these three techniques suffer from the multi-path environment, in which the LoS (Line of Sight) component does not necessarily dominate over other NLoS (Non Line of Sight) counterparts. Thus, most technically available ranging is based on received signal strength; in fact, RSSI (Received Signal Strength Indication) is widely used in wireless communications to provide distance estimation [45].

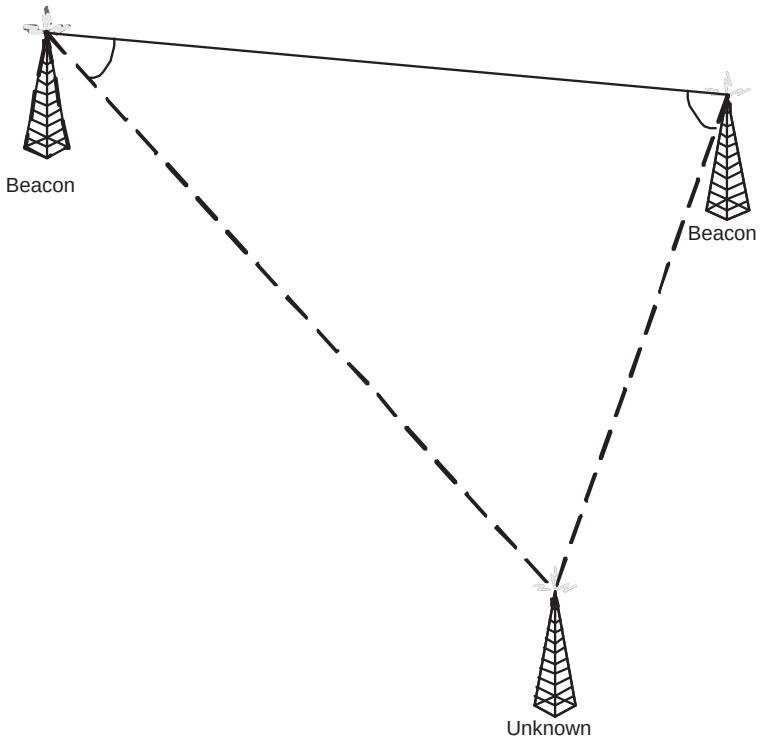

Figure 1.3. AOA ranging.

The underlying observation is that the average large-scale path loss can be expressed as a function of distance by using a path loss exponent, n [23].

$$\bar{PL}(d) = \bar{PL}(d_0)(\frac{d}{d_0})^n \tag{1.1}$$

where n is the path loss exponent, which indicates the rate at which the path loss increases with distance, d_0 is the close-in reference distance, which is determined from measurement close to the transmitter, and d is the distance from the source to the receiving point. Measurements have also shown that at any value of d, the path loss $PL(d)$ at a particular location is random and distributed log-normally (normal in dB) about the mean distance-dependent value [46–48].

$$PL(d)[dB] = \bar{PL}(d)[dB] + X_\sigma, \tag{1.2}$$

where X_σ is a zero-mean Gaussian distributed random variable (in dB) with standard deviation σ (also in dB). The log-normal shadowing is the main source of distance error for received-signal-strength-based ranging methods. The values of n and σ are often

estimated empirically, for example, n could vary from 2 to 10 for different environments, and typical value of σ in urban area is around 10 dB [49–51].

Due to the log-normal shadowing, the RSS-based ranging could be very rough. For example, the median localization error of commodity 802.11 technology is $10ft$ [52], such accuracy may be achieved by alternative techniques, for example, exploiting the dense deployment to estimate distance between nodes. For those applications where the sensor nodes are over-densely deployed, the distance between the nodes are short and the variance of such distance is also small. Therefore, it is quite promising to estimate the end-to-end distance based on the number of hops [53–55].

1.3 UnderWater Acoustic Sensor Network

An UnderWater Acoustic Sensor Network (UW-ASN) can be thought of as an *ad hoc* network consisting of sensors linked by an acoustic medium to perform distributed sensing tasks [56–58]. To achieve this objective, sensors must self-organize into an autonomous network which can adapt to the characteristics of the underwater environment. UW-ASNs share many communication technologies with traditional *ad hoc* networks and terrestrial wireless sensor networks, but there are some vital differences such as limited energy and bandwidth constraint [59–65], thus the protocols developed for traditional wireless ad hoc networks are not necessarily well suited to the unique features of WSNs [66]. When a wireless sensor may have to operate for a relatively long duration on a tiny battery, energy efficiency becomes a major concern.

Another issue in shallow water communications is that due to the limit of bandwidth in shallow water communications [67, 68], multi-hop communication could introduce heavy interference between cluster members, therefore, each sensor in a cluster communicate directly to its cluster head and intra-cluster communication should be coordinated by the cluster head in order to maximize the bandwidth usage.

1.4 Deployment Issue

Our study is based on random node distribution, but even for those applications where nodes are manually placed, there is room for randomness. Especially in underwater environment, where sensor nodes can easily be moved out of desired places due to water current caused by wind, tide, animal and human activities, failing to take into consideration the deployment randomness might leave more room for errors. Furthermore, unlike their terrestrial counterparts where sensor nodes are often deployed on the terrain surface, the underwater sensor nodes are often deployed along a line around bays and harbors to maximize the detection of ship traffic in the naturally constrained waterway [69]. In addition, some underwater sensor nodes are able to adjust their depth to better the network coverage. Therefore, it is necessary to consider the effect of 1-D, 2-D and 3-D random deployment on the clustering.

1.5 Dissertation Structure

This dissertation begin with a general discussion of energy efficiency in wireless sensor networks. Chapter 2 also includes the data correlation model that our research is based on. Chapter 3 discusses the optimal cluster size for terrestrial wireless sensor networks and proposes a self-organization scheme to achieve the desired clustering. Chapter 4 models the hop-distance relationship in wireless sensor networks and propose a new ranging method. Chapter 5 studies the mirror problem and comes up with a novel estimation, which can be used to improve resource allocation. Chapter 6 extends the clustering study to underwater acoustic sensor networks. Chapter 7 concludes this dissertation.

CHAPTER 2

BACKGROUND

2.1 Review of Wireless Medium Access

Many special flavored MAC protocols have been proposed for WSN for energy efficiency, less latency or higher throughputBao02, Elson01, Kanodia02, Mill05, Raje03, Schu02, Sing98. In this paper, we consider a generic MAC that is compatible with the basic access mechanism described in 802.11 DCF [70]. As illustrated in Fig. 2.1, after the channel is sensed idle for greater than or equal to a DIFS(Distributed InterFrame Spacing) period, the transmitting node generates a random backoff timer chosen uniformly from the range $[0, w-1]$, where w is the size of contention window. In a binary exponential backoff scheme, the value of w is reset to CW_{min} after each successful transmission, and doubled after each unsuccessful transmission, up to CW_{max} (maximum contention window). The backoff timer is decrement

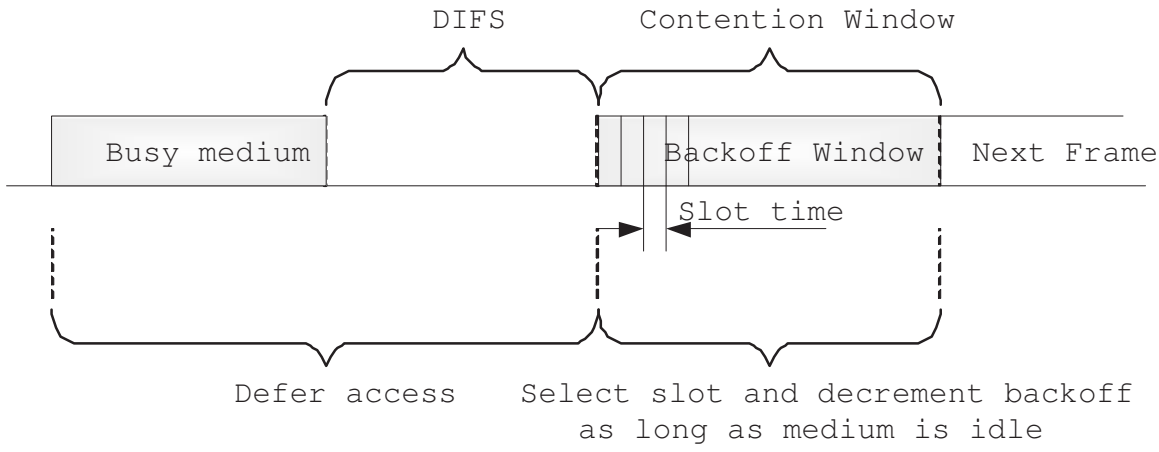

Figure 2.1. A generic MAC.

The collisions of packets in the contention-based MAC generally degrade channel utilization and increase energy consumption, which motivates establishing transmission

schedules to allow nodes to communicate without collisions. In NAMA (Node Activation Multiple Access) [71] and TRAMA (Traffic-Adaptive Medium Access protocol) [72], a distributed election scheme is used to determine which node can transmit at a particular time slot. From this point of view, LEACH is also a schedule-based scheme, in which cluster formation is a random-access period to establish a scheduled-access period collision-free (Fig. 2.2).

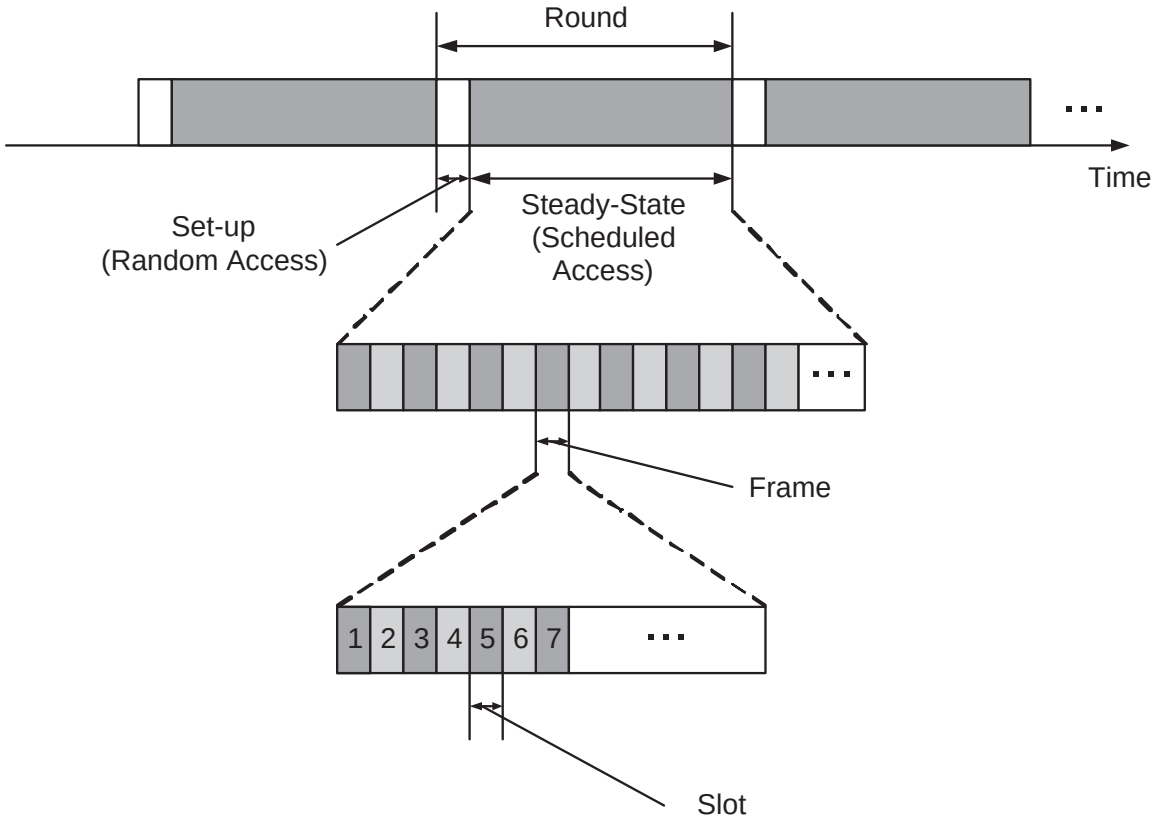

Figure 2.2. Time line showing LEACH's frame structure.

2.2 Radio Energy Consumption

The following model is adopted from [35] where perfect power control is assumed. To transmit l bits over distance d, the sender's radio expends

$$E_{TX}(l,d) = \begin{cases} lE_{elec} + l\epsilon_{fs}d^2 & d < d_0 \\ lE_{elec} + l\epsilon_{mp}d^4 & d \geq d_0 \end{cases} \tag{2.1}$$

and the receiver's radio expends

$$E_{RX}(l,d) = lE_{elec}. \tag{2.2}$$

E_{elec} is the unit energy consumed by the electronics to process one bit of message, ϵ_{fs} and ϵ_{mp} are the amplifier factor for free-space and multi-path models, respectively, and d_0 is the reference distance to determine which model to use. The values of these communication energy parameters are set as in Table 2.1.

Table 2.1. Communication Energy Parameters

Name	Value
d_0	86.2m
E_{elec}	$50nJ/bit$
E_{DA}	$5nJ/bit$
ϵ_{fs}	$10pJ/bit/m^2$
ϵ_{mp}	$0.0013pJ/bit/m^4$

2.3 Data Correlation Model

The data collected by neighboring sensors have a lot of redundancy, thus, [35] assumes perfect data correlation that all individual signals from members of the same cluster can be combined into a single representative signal. Nevertheless, this assumption cannot hold when the cluster size increases to some extent. Therefore, we develop a complementary exponential data correlation model based on the observations in distributed data compression [73–76].

Considering the phenomenon of interest as a random process, the correlation between data collected by two sensors is generally a decreasing function of the distance r between them. After the data aggregation removes most of the redundancy, the residue can be assumed to be an increasing function of r. Based on the above observation, the data aggregation effect is modeled as below.

Suppose there are M_k non-head members in cluster k ($k = 1, 2, 3, ..., c$), the ith member ($i = 1, 2, 3, ..., M_k$) collects l bits and sends them back to its head k at distance r_{ki}, the head expends $2lE_{DA}$ Joules on the data aggregation of the $2l$ bits (l bits collected by itself and another l bits by its ith member), where E_{DA} is set as $5nJ/bit$ as in [35] and listed in Table 2.1. The resulting data is assumed of $l(1+\eta_{ki})$ bits, where η_{ki} is data aggregation residue ratio and assumed to be complementary exponential, specifically,

$$\eta_{ki} = 1 - e^{-\alpha r_{ki}}, 0 < \alpha < 1, \tag{2.3}$$

where α is a small positive real number whose magnitude depends on specific phenomenon of interest. For example, the light, acoustic, seismic and thermal signals often show a strong correlation at short distance, and thus, α will have smaller values for such data. Since η is a monotonically decreasing function of α and r, η approaches zero for smaller α and r. This model can approach the perfect-data-correlation assumption in [35] by decreasing α or approach the no-data-aggregation assumption in [12, 13] by increasing α, thus, different scenarios can easily be set up by varying α.

2.4 LEACH

LEACH uses CDMA-TDMA hybrid communication scheme [77]. Each cluster has its own Spread Spectrum code so that the interference between clusters is minimized. For intra-cluster communications, TDMA slots are assigned for each member to minimize media contention. The operation of LEACH is divided into rounds. At the beginning of each round, cluster heads are elected and other nodes join them as members so that N nodes are partitioned into c clusters. When a cluster is formed, the cluster head creates and

broadcasts a time schedule to its members. As shown in Fig.2.2, each member is assigned a time slot per frame to send its data to its cluster head, and then the cluster head performs data aggregation and sends the resulting data back to the base station. Compared with multi-hop routing schemes, LEACH shows an outstanding energy efficiency, which is referred to as clustering energy gain in the following. Using a low duty-cycle, LEACH could also take advantage of relaxtion effect of batteries [78].

However, there are two drawbacks in LEACH's cluster formation:

a. **Dependence on Global Information** In LEACH, each node i elects itself to be a cluster head at the beginning of round $r+1$(which starts at time t) with probability $P_i(t)$. Two ways were used to determine the self-electing probability $P_i(t)$ in [35]. If all nodes are assumed to start with an equal amount of energy, $P_i(t)$ is given by

$$P_i(t) = \begin{cases} \frac{c}{N - c*(r mod \frac{N}{c})} & : C_i(t) = 1 \\ 0 & : C_i(t) = 0 \end{cases}, \tag{2.4}$$

where c is the desired number of clusters and $C_i(t)$ is the indicator function determining whether or not node i has been a cluster head in the most recent ($r \ mod \ (N/c)$) rounds. The more general estimate of $P_i(t)$ is given by

$$P_i(t) = min\{\frac{E_i(t)}{E_{total}(t)}c, 1\}, \tag{2.5}$$

where $E_i(t)$ is the current energy(i.e. remaining battery capacity) of node i and

$$E_{total}(t) = \sum_{i=1}^{N} E_i(t). \tag{2.6}$$

Essentially, N in (2.4) and E_{total} in (2.5) are global information, which is only accessible via other routing schemes.

b. **Random Election** Although random decision generally strengthens the robustness by avoiding sticking to a single choice, too much randomness may shift the decision away from the optimal range. In LEACH's case, suppose (2.5) is used and

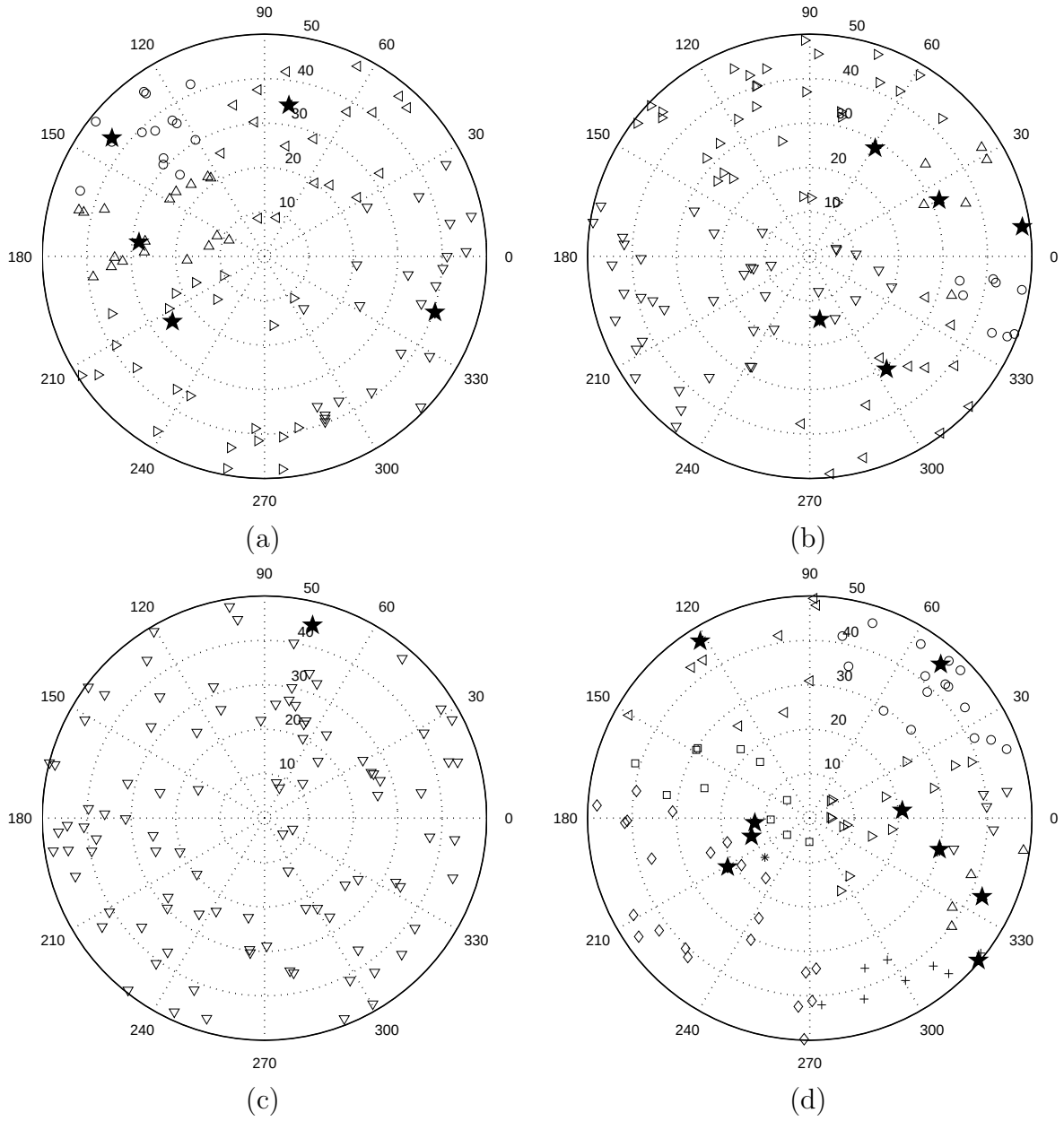

Figure 2.3. 100 nodes elect 5 heads (Heads marked by pentagrams).(a) Five heads are elected and evenly distributed. (b) Five heads are elected and clump in the right semi-circle. (c) Only one head is elected. (d) Nine heads are elected.

all nodes have equal amount of energy, if N nodes want to elect c heads among them, then the self-electing probability for each node is

$$p = \frac{c}{N} \tag{2.7}$$

Then the probability of "n heads are elected" is

$$Pr(n \text{ elected heads}) = \binom{N}{n} p^n (1-p)^{(N-n)} \tag{2.8}$$

The distribution of the number of elected heads is listed in Table 2.2. Obviously, too few (Fig. 2.3(c)) and too many (Fig. 2.3(d)) elected heads would damage the energy efficiency. Moreover, in the case of "no elected head" whose probability listed in row 1, all the nodes have to communicate directly with the base station, in which case all the clustering energy gain is lost. When the number of elected heads is too few, for example, only one head is elected, the head may be exhausted by the tremendous data sent to it. In such cases, the energy efficiency is tremendously compromised. Another problem introduced by the random head selection is that

Table 2.2. Outcome of 100 nodes electing 5 heads.

n: number of elected heads	$Pr(n$ elected heads$)$
0	0.0059
1	0.0312
2	0.0812
3	0.1396
4	0.1781
5	0.1800
6	0.1500
7	0.1060
8	0.0649
9	0.0349
≥ 10	0.0341

the sensor locations are not taken into consideration. Obviously, the even layout of heads would favor energy efficiency (Fig. 2.3(a)). When heads are randomly selected as in LEACH, elected heads sometimes clump together as shown in Fig. 2.3(b), which leads to unnecessary energy waste.

2.5 Hop-Distance Relation

Both APS [53] and Hop-TERRAIN [55] find the number of hops from a node to each of the anchors and then multiply this hop count by a shared metric (average single-hop distance) to estimate the range between the node and each anchor. The known positions of anchor nodes and these computed ranges are then used to perform a triangulation to obtain estimated node positions. A further refinement phase is proposed in [55], which uses least squares on local computation. However, as we show later, the distance does not increase linearly with the number of hops. Therefore, a better knowledge about the hop-distance relationship can cast new light on distance estimation.

In [79], Hou and Li studied the 2-D Poisson distribution to find an optimal transmission range. They found that the hop-distance distribution is determined not only by node density and transmission range but also by the routing strategy. They showed results for three routing strategies, Most Forward with Fixed Radius, Nearest with Forward Progress, and Most Forward with Variable Radius. Cheng and Robertazzi in [80] studied the one-dimension Poisson point and found the pdf of r_i and the dependency of r_i on previous r_j, $j < i$. They also pointed out the 2-D Poisson point distribution is analogous to the 1-D case, replacing the length of the segment by the area of the range.

Vural and Ekici re-examined the study under the sensor networks circumstances in [81], and gave the mean and variance of multi-hop distance for 1-D Poisson point distribution. They also proposed to approximate the multi-hop distance using Gaussian. Zorzi and Rao derive the mean number of hops of the minimal hop-count route through simulations and analytic bounds in [82]. Chandler [83] derives an expression for t-hop outage probability for 2-D Poisson node distribution. However, Mukherjee and Avidor [84] argue that one of Chandler's assumptions is flawed and thus his expression is in fact a lower bound on the desired probability. They also rigorously derive the pdf of the minimal number of hops for a given distance in a fading environment. Although the exact analytic results are available in the literature, their monstrous computational complexity limits their applications. Therefore, we try to approximate the hop-distance

relation and simplify the decision process and error analysis in this paper. Considering the application of resource allocation, only large-scale path loss is considered and thus the fading is ignored.

2.6 Skewness and Kurtosis

Skewness is a measure of symmetry, or more precisely, the lack of symmetry. A distribution, or sample set, is symmetric if it looks the same to the left and right of the center point.

Definition 1 *[85] For a given sample set X,*

$$m_3 = \Sigma(X - \bar{X})^3/n, \tag{2.9}$$

$$m_2 = \Sigma(X - \bar{X})^2/n, \tag{2.10}$$

where $\bar{X}$ is the sample mean of X, and n is the size of X. Then a sample estimate of skewness coefficient *is given by*

$$g_1 = \frac{m_3}{m_2^{\frac{3}{2}}}. \tag{2.11}$$

Skewness is zero for a symmetric distribution. Positive skewness indicates right skewness and negative indicates left.

Kurtosis is a measure of whether the data are peaked or flat relative to a normal distribution.

Definition 2 *[85] A sample estimate of kurtosis for a sample set X is given by*

$$g_2 = m_4/m_2^2 - 3, \tag{2.12}$$

where $m_4 = \Sigma(X - \bar{X})^4/n$ is the fourth-order moment of $\bar{X}$ about its mean.

Skewness and kurtosis is useful in determining whether a sample set is normal. Note that the skewness and kurtosis of a normal distribution are both zero; significant skewness and kurtosis clearly indicate that data are not normal.

2.7 Chi-Square Test

Chi-square test is widely used to determine the goodness of fit of a distribution to a set of experimental data. It works as follows:

- 1. Partition the sample space into the union of K disjoint intervals.
- 2. Compute the probability b_k that an outcome falls in the kth interval under the postulated distribution. Then $m_k = nb_k$ is the expected number of outcomes that fall in the kth interval in n repetitions of the experiment.
- 3. The chi-square statistic is defined as the weighted difference between the observed number of outcomes, N_k, that fall in the kth interval, and the expected number m_k.

$$D^2 = \Sigma_{k=1}^{K} \frac{(N_k - m_k)^2}{m_k} \tag{2.13}$$

- 4. The hypothesis is rejected if $D^2 \geq t_\alpha$, where t_α is a threshold determined by a given significance level. Otherwise, the fit is considered good.

2.8 Underwater Acoustics Fundamentals

Based on the data and formulas in [69], Jurdak, Lopes and Baldi [86] derived the following model,

$$SL = TL + 85, \tag{2.14}$$

where SL is the source level and TL is the transmission loss. All the quantities in (2.14) are in $dB\ re\ \mu Pa$, where the reference value of 1 μPa amounts to $0.67 \times 10^{-22} Watts/cm^2$. For cylindrically spread signals, the transmission loss is approximated by [69],

$$TL = 10 \log d + \alpha d \times 10^{-3}, \tag{2.15}$$

where d is the distance between source and receiver in meters, α is the frequency dependent medium absorption coefficient. Fisher and Simmons [87] measured the medium

absorption in shallow seawater at temperatures at $4Cand20$C. The average is obtained in [86],

$$\bar{\alpha} = \begin{cases} 0.0601 \times f^{0.8552} & 1 \le f \le 6 \\ 9.7888 \times f^{1.7885} \times 10^{-3} & 7 \le f \le 20 \\ 0.3026 \times f - 3.7933 & 20 \le f \le 35 \\ 0.504 \times f - 11.2 & 35 \le f \le 50. \end{cases} \tag{2.16}$$

To guarantee the reception quality, the required threshold of α, denoted by $\tilde{\alpha}$, might be chosen larger than $\bar{\alpha}$. However, we can generally expect $\tilde{\alpha}$ be a monotonically decreasing function of frequency f. To emphasize their relationship, $\tilde{\alpha}$ is written as $\tilde{\alpha}(f)$ in the rest of this paper. The transmitter power P_t required to achieve an intensity I_t at a reference distance of $1m$ is expressed as,

$$P_t = 2\pi \times 1m \times H \times I_t, \tag{2.17}$$

where I_t is related to SL by

$$I_t = 10^{SL/10} \times 0.67 \times 10^{-18}. \tag{2.18}$$

Summing up (2.14), (2.15), (2.17) and (2.18), we obtain

$$P_t = CHde^{a(f)d}, \tag{2.19}$$

$$C \triangleq 2\pi(0.67)10^{-9.5}$$

$$a(f) \triangleq 0.001\alpha(f)\ln 10 \tag{2.20}$$

where H is the water depth in meters.

Therefore, to transmit l bits over distance d, the sender's radio expends

$$E_{TX}(l,d) = lE_{elec} + lT_bCHde^{a(f)d} \tag{2.21}$$

and the receiver's radio expends

$$E_{RX}(l,d) = lE_{elec}, \tag{2.22}$$

where T_b the bit duration, E_{elec} is the unit energy consumed by the electronics to process one bit of message.

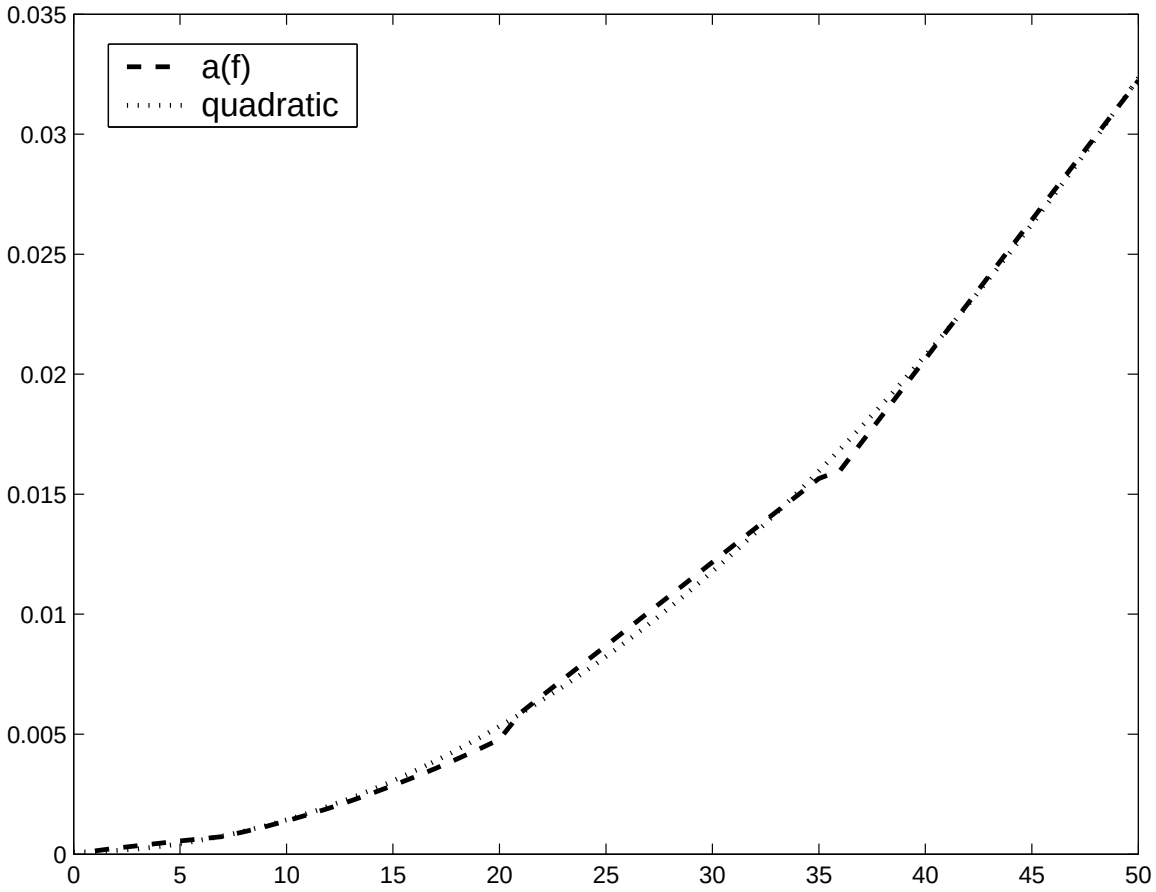

Figure 2.4. Plot of $a(f)$.

CHAPTER 3

CLUSTERING FOR TERRESTRIAL WSN

3.1 Optimal Clustering

In this section, we make data-centric analysis of energy consumption in WSN and propose a new criterion, which is the theoretical basis of Medium-Contention Based ClusterHeadship Auction.

3.1.1 Problem Formulation

Clustering has been widely used in pattern recognition [88], and we use it to obtain the energy-efficient organization for WSN. From the data-centric view [89], the data collected by a node can be sent back directly to the base station or relayed by a cluster head. The first case occurs if this node is a cluster head; the data collected by head k is data-aggregated (with the data collected by its members) and sent back to the base station. Thus, the energy cost for each bit of data collected by head k is

$$J_{CH(k)} = E_{DA} + E_{elec} + \epsilon_{mp} d_k^4, \tag{3.1}$$

where d_k is the distance between head k and the base station.

For the second case, consider non-head member ki, the ith sensor in cluster k, with distance r_{ki} to its cluster head, member ki sends its data to head k, and then head k performs data aggregation on the data and sends the resulting data to the base station. Thus, the energy cost for each bit of data collected by non-head member ki is

$$J_{CM(ki)} = E_{elec} + \epsilon_{fs} r_{ki}^2 + E_{elec} + E_{DA} + \eta(r_{ki})(E_{elec} + \epsilon_{mp} d_k^4), \tag{3.2}$$

where $\eta(r_{ki})$ is the data aggregation residue ratio introduced in Section 2.3.

Considering all c clusters, the overall cost is

$$J_{total} = \sum_{k=1}^{c} \{J_{CH(k)} + \sum_{i=1}^{M_k} J_{CM(ki)}\}, \tag{3.3}$$

where M_k is the number of non-head members in cluster k.

Taking $E[J_{total}]$ the expected value of the overall energy cost as the objective function, the original problem is translated into an objective function clustering. If a central control scheme is possible, an iterative algorithm can be run at the base station to minimized $E[J_{total}]$. For example, Fuzzy c-Means is utilized in [90] to minimize a Euclidean-distance-based functional representing the energy cost in Wireless Personal Area Networks. However, since WSNs are working in *ad hoc* mode, clustering decision must be distributed to each sensor node. Thus, our goal is using only local information to achieve energy-efficient clustering.

3.1.2 Influence Range

Generally, if a node is close to a cluster head, there is some energy gain if it joins that cluster. The energy gain diminishes when the distance between the non-head member and the head increases. Consequently, the energy gain approaches zero at some critical distance, termed as influence range. To determine the influence range, consider a node i with a head k at distance r. The node could choose to be a non-head member or a head, which would consequently cost J_{CM} or J_{CH} as in (3.2) and (3.1). Naturally, the decision should be based on the comparison of J_{CM} and J_{CH} as

$$J_{CM} \underset{CM}{\overset{CH}{\gtrless}} J_{CH}, \tag{3.4}$$

i.e., the decision rule for each sensor is:

$$\text{Node } i \text{ elects to be } \begin{cases} \text{a non-head member} & \text{if } J_{CM} < J_{CH} \\ \text{a cluster head} & \text{if } J_{CM} > J_{CH} \end{cases} \tag{3.5}$$

We call this criterion as local energy efficiency criterion, because it is based on only the local information. Substituting (3.1) and (3.2) into (3.4), we obtain

$$\begin{aligned} E_{elec} + \epsilon_{fs} r_{ik}^2 + E_{elec} + E_{DA} + \eta(r_{ik})(E_{elec} + \epsilon_{mp} d_k^4) \\ \underset{CM}{\overset{CH}{\gtrless}} E_{DA} + E_{elec} + \epsilon_{mp} d_i^4. \end{aligned} \tag{3.6}$$

The influence range can be obtained by equating two sides though a closed form may be unavailable. Obviously, the cluster radius R_c has to be much smaller than the influence range because the energy gain is so low at the outer ring that a new cluster be formed. Although this criterion is too complex to be used in real applications, it promotes using R_c instead of c as the clustering objective parameter to guide the election. Denote the areas occupied by the whole WSN and the cluster by S_N and S_c respectively,

$$c \approx \frac{S_N}{S_c}. \tag{3.7}$$

Assume S_N and S_c are both circular, R_c is related to c by

$$c = \frac{\pi R^2}{\pi R_c^2} = (\frac{R}{R_c})^2, \tag{3.8}$$

where R is the radius of S_N. Although it is mathematically equivalent to partition nodes into c clusters or to organize nodes into clusters with radius R_c, the former is definitely a global approach, which leads to dependence on the global information. Thus, the latter is more suitable for a distributed algorithm.

3.1.3 Optimal Cluster Size

As indicated in (3.8), it is equivalent to determine c or R_c. Here, we try to analytically determine the optimal value of c using the introduced models. LEACH can only determine a rough range $c_{opt} \in [1, 6]$ for a similar 100-node network [35], while our analysis predicts the optimal value of R_c in simulation with satisfying accuracy.

The typical scenario is that N nodes are distributed uniformly in a circular region with radius R. There are c clusters with one cluster head and $n-1$ non-head members within each cluster. n is the average number of cluster members and related to c by

$$n \approx N/c. \tag{3.9}$$

Based on (3.3), the average total energy cost can be approximated by

$$\begin{aligned} \bar{J}_{total} &= c(\bar{J}_{CH} + (n-1)\bar{J}_{CM}) \\ &= c\bar{J}_{CH} + (N-c)\bar{J}_{CM} \end{aligned} \tag{3.10}$$

where $\bar{J}_{CH}$ and $\bar{J}_{CM}$ are the average energy cost for the cluster head and non-head member respectively.

Following (3.1) and (3.2),

$$\bar{J}_{CH} = E_{DA} + E_{elec} + \epsilon_{mp} E[d^4], \tag{3.11}$$

$$\bar{J}_{CM} = E_{elec} + \epsilon_{fs} E[r^2] + E_{elec} + E_{DA} + E[\eta(r)(E_{elec} + \epsilon_{mp} d^4)]. \tag{3.12}$$

Since all nodes are independently deployed, r and d are independent, thus, (3.12) can be written as

$$\bar{J}_{CM} = E_{elec} + \epsilon_{fs} E[r^2] + E_{elec} + E_{DA} + E[\eta(r)](E_{elec} + \epsilon_{mp} E[d^4]). \tag{3.13}$$

We estimate the expected values in (3.11) and (3.13) as follows. Assuming the cluster head is at the center of mass of the cluster,

$$\begin{aligned} E[r^2] &= \int\int_{S_c} r^2 \rho_c(r,\theta) r dr d\theta \\ &= \int_0^{2\pi} \int_0^{R_c} r^2 \rho_c(r,\theta) r dr d\theta \end{aligned} \tag{3.14}$$

where $\rho_c(r,\theta)$ is the node distribution density. Since the nodes are assumed to be uniformly distributed, $\rho_c(r,\theta)$ is a constant given by

$$\rho_c = 1/\pi R_c^2 = c/(\pi R^2). \tag{3.15}$$

Substituting (3.15) and (3.8) into (3.14),

$$\begin{aligned} E[r^2] &= \frac{\pi \rho_c R_c^4}{2} \\ &= \frac{R^2}{2c} \end{aligned} \tag{3.16}$$

Similarly,

$$\begin{aligned} E[\eta(r)] &= \int\int_{S_c}(1-e^{-\alpha r})\rho_c(r,\theta)rdrd\theta \\ &= \frac{c}{\pi R^2}\int_0^{2\pi}\int_0^{R_c}(1-e^{-\alpha r})rdrd\theta \\ &= \frac{2c}{R^2}\int_0^{R_c}(1-e^{-\alpha r})rdr \qquad (3.17) \\ &= 1+\frac{2c}{\alpha^2R^2}(e^{-\frac{\alpha R}{\sqrt{c}}}(\frac{\alpha R}{\sqrt{c}}+1)-1) \qquad (3.18) \end{aligned}$$

$$\begin{aligned} E[d^4] &= \int\int_{S_N}|r-r_{BS}|^4\rho_N(r,\theta)rdrd\theta \\ &= \frac{1}{\pi R^2}\int_0^{2\pi}\int_0^{R}(r^2+r_{BS}^2-2rr_{BS}cos(\theta-\theta_{BS}))^2rdrd\theta \qquad (3.19) \end{aligned}$$

Since $E[d^4]$ is a function of R and irrelevant to c, we keep it in the further derivation.

The optimal value of c can be obtained by setting $\frac{\partial \bar{J}_{total}}{\partial c}$ to zero.

$$\begin{aligned} \frac{\partial \bar{J}_{total}}{\partial c} &= \bar{J}_{CH}-\bar{J}_{CM}+(N-c)\frac{\partial \bar{J}_{CM}}{\partial c} \\ &= \epsilon_{mp}E[d^4]-E_{elec}-\epsilon_{fs}\frac{R^2}{2c}-E[\eta(r)](E_{elec}+\epsilon_{mp}E[d^4]) \\ &\quad +(N-c)(-\frac{\epsilon_{fs}R^2}{2c^2}+\frac{\partial E[\eta(r)]}{\partial c}(E_{elec}+\epsilon_{mp}E[d^4])), \qquad (3.20) \end{aligned}$$

$$\begin{aligned} \frac{\partial^2 \bar{J}_{total}}{\partial c^2} &= \frac{\epsilon_{fs}R^2}{2c^2}-\frac{\partial E[\eta(r)]}{\partial c}(E_{elec}+\epsilon_{mp}E[d^4]) \\ &\quad -(-\frac{\epsilon_{fs}R^2}{2c^2}+\frac{\partial E[\eta(r)]}{\partial c}(E_{elec}+\epsilon_{mp}E[d^4])) \\ &\quad +(N-c)(\frac{\epsilon_{fs}R^2}{c^3}+\frac{\partial^2 E[\eta(r)]}{\partial c^2}(E_{elec}+\epsilon_{mp}E[d^4])) \\ &= \frac{\epsilon_{fs}R^2}{c^2}+(N-c)\frac{\epsilon_{fs}R^2}{c^3} \\ &\quad -2\frac{\partial E[\eta(r)]}{\partial c}(E_{elec}+\epsilon_{mp}E[d^4]) \\ &\quad +(N-c)\frac{\partial^2 E[\eta(r)]}{\partial c^2}(E_{elec}+\epsilon_{mp}E[d^4]) \qquad (3.21) \end{aligned}$$

where $\frac{\partial E[\eta(r)]}{\partial c}$, $\frac{\partial^2 E[\eta(r)]}{\partial c^2}$ can be computed based on (3.18).

$$\frac{\partial E[\eta(r)]}{\partial c}=\frac{2}{\alpha^2R^2}(e^{-\frac{\alpha R}{\sqrt{c}}}(\frac{\alpha R}{\sqrt{c}}+1)-1)+\frac{e^{-\frac{\alpha R}{\sqrt{c}}}}{c} \qquad (3.22)$$

$$\frac{\partial^2 E[\eta(r)]}{\partial c^2} = \frac{\alpha R e^{-\frac{\alpha R}{\sqrt{c}}}}{2c^{5/2}} \tag{3.23}$$

Since it is impossible to solve (3.20) algebraically, we turn to the numerical solution. For example, the base station is located at $(r_{BS}, \theta_{BS}) = (125, 0)$ and $N = 100$, $R = 50m$ in our experiments, we can evaluate (3.19) as

$$E[d^4] = 5.8997e + 008. \tag{3.24}$$

In Fig.3.1(a)(b), we plot $\frac{\partial \bar{J}_{total}}{\partial c}$ over c for $\alpha = 0.001$ and $\alpha = 0.05$ respectively.

The corresponding c_{opt} can be easily obtained by setting $\frac{\partial \bar{J}_{total}}{\partial c} = 0$.

$$c_{opt} = \begin{cases} 1.6569, & \text{for } \alpha = 0.001 \\ 20.2600, & \text{for } \alpha = 0.05 \end{cases} \tag{3.25}$$

Note that $\frac{\partial^2 \bar{J}_{total}}{\partial c^2} \mid_{c_{opt}=1.6569} = 2.98E-7 > 0$ and $\frac{\partial^2 \bar{J}_{total}}{\partial c^2} \mid_{c_{opt}=20.26} = 2.51E-9 > 0$, which indicates $\bar{J}_{total}$ is minimized at these c_{opt}'s. According to (3.8), the corresponding R_c is

$$R_c = \begin{cases} 38m, & \text{for } \alpha = 0.001 \\ 11m, & \text{for } \alpha = 0.05 \end{cases} \tag{3.26}$$

We are also interested in the relation of N to c_{opt}. In Fig.3.2(a)(b), we plot c_{opt} over N for $\alpha = 0.001$ and $\alpha = 0.05$ respectively. These figures show that c_{opt} is an increasing function of N, which indicates the clustering objective parameter (c or R_c) should be adjusted adaptively if N varies.

3.2 Medium-Contention Based ClusterHeadship Auction

Medium-Contention Based ClusterHeadship Auction (MCCHA) is designed to replace the cluster formation occurring at the beginning of each round in LEACH. In MCCHA, there is no global broadcast. As shown in Fig.3.3, each node firstly broadcasts its vital information at the maximum radio power level so that the knowledge is spread as widely as possible. Such "maximum-power" broadcasts are not frequent in MCCHA,

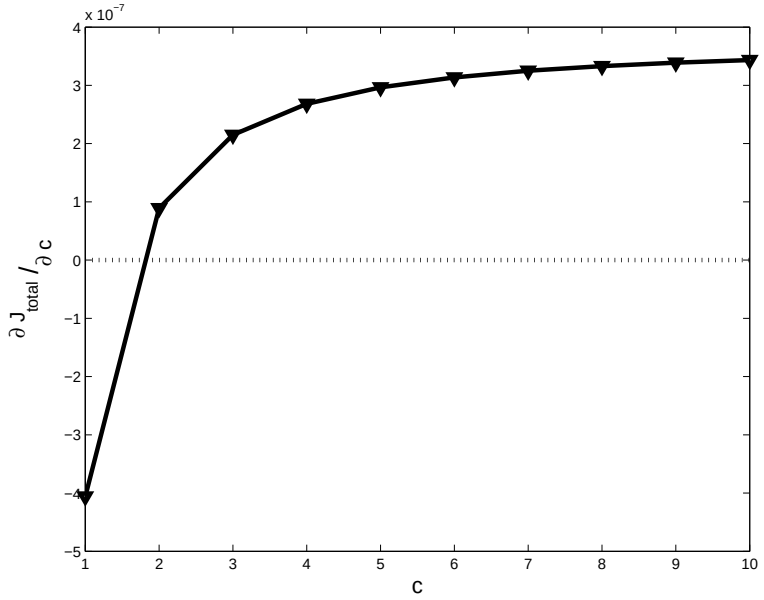

(a)

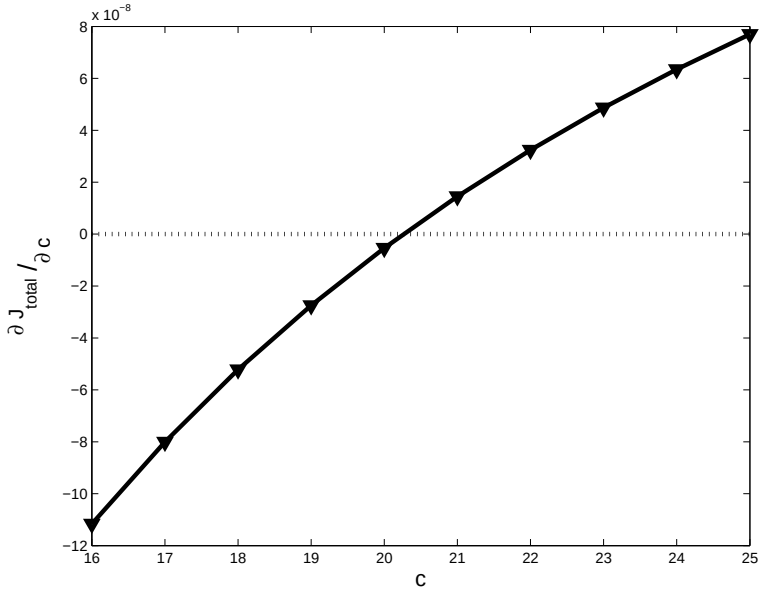

(b)

Figure 3.1. Plot of $\frac{\partial \bar{J}_{total}}{\partial c}$ for $N = 100$, $R = 50m$ and $(r_{BS}, \theta_{BS}) = (125, 0)$.(a)$\alpha = 0.001$. (b)$\alpha = 0.05$.

which helps the energy efficiency. The vital information may include nodes' energy, location, etc., though only energy information is needed by MCCHA. Then, each node counts its neighbors and broadcasts the number of its neighbors at an adjusted power level corresponding to the cluster radius R_c. The cluster radius R_c is an important system parameter for energy efficiency. As shown in Section 3.1.3, given a specific type of

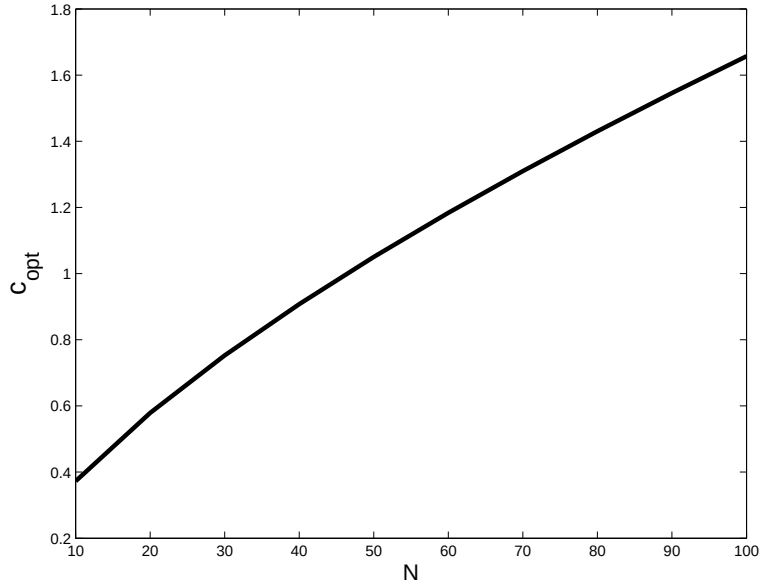

(a)

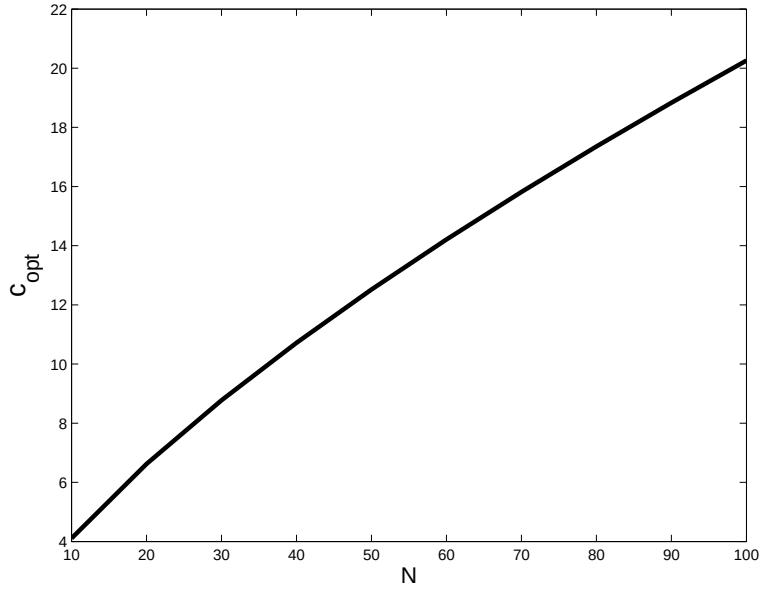

(b)

Figure 3.2. Plot of c_{opt} vs. N for $R = 50m$ and $(r_{BS}, \theta_{BS}) = (125, 0)$.(a)$\alpha = 0.001$. (b)$\alpha = 0.05$.

application, R_c is mainly determined by the node density. In MCCHA, each node should choose an appropriate R_c according the neighbor count in its transmission range, which is a good estimator of the local density.

If a node's headship potential *qualifies* as a head compared to its neighbors', it will try to claim the headship by broadcasting locally, which can be viewed as placing

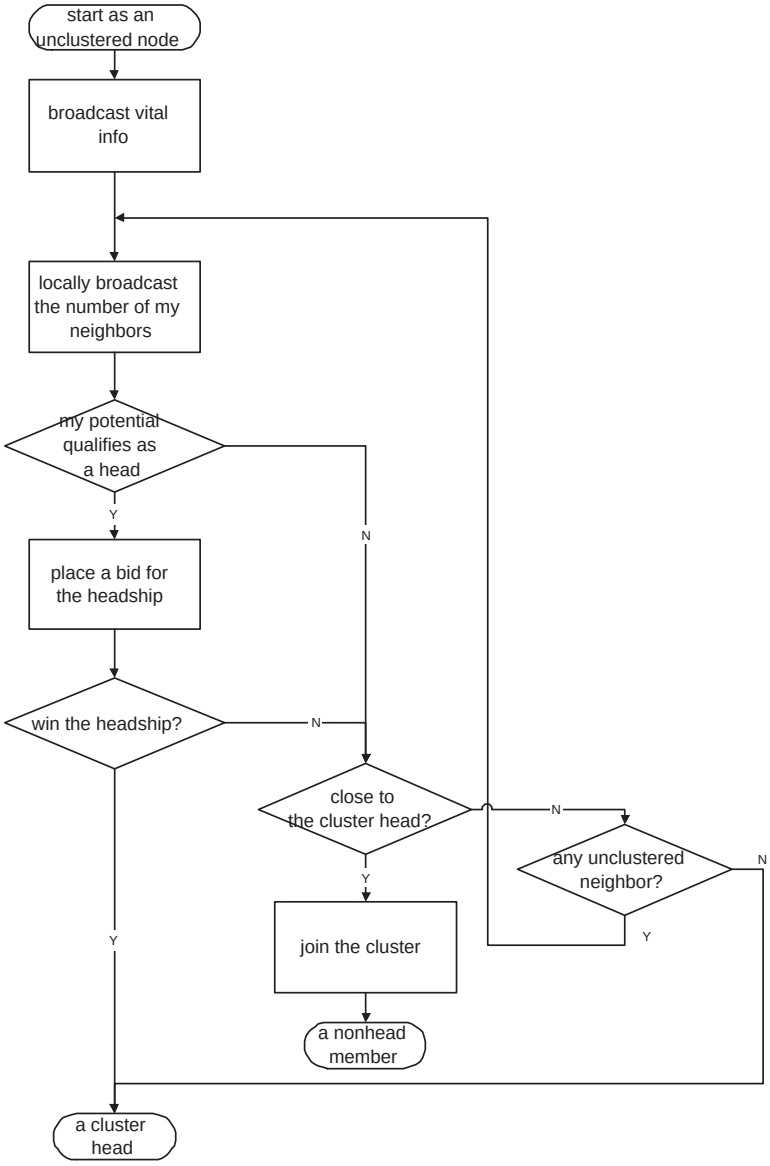

Figure 3.3. Flow chart of a node in MCCHA.

a bid for the headship. A node's "neighbors" are defined as the nearby nodes within distance R_c from that node. Due to the possible contention for the headship, such bids could fail, which is indicated by the collision of "headship claims". Using the modified MAC described below, the bidders will contend with each other until a node with satisfactory potential wins. By doing so, the head-to-be expels other possible heads in its neighborhood, and in consequence, the clusters with desired size are formed.

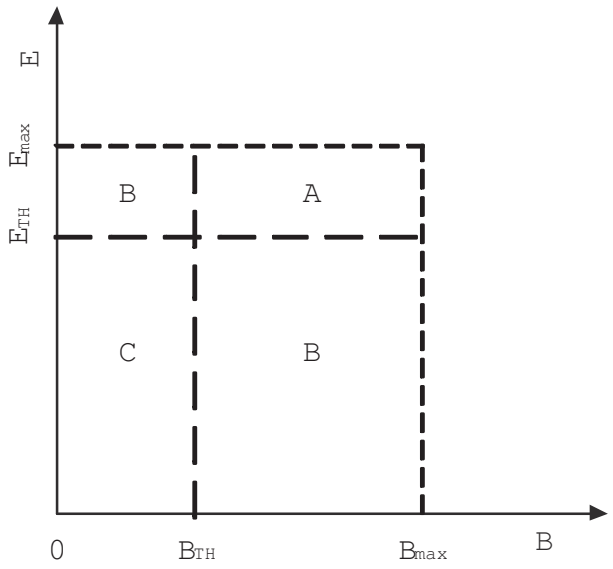

Figure 3.4. Categories of bidders.

The headship potential is an important parameter, which replaces the self-electing probability used in native LEACH. As discussed in [35], the node's energy is important to determine its potential because the headship can be rotated among nodes by assigning more potential to the nodes with higher energy. In addition, we propose taking the number of neighbors into consideration, because the energy gain is prominent only in the neighborhood of the head as shown in Section 3.1.2 and thus it is energy-efficient to let the node with more neighbors win the headship.

Based on these considerations, the qualification conditions are set as below. For any node, let $\mathcal{N}$ denote the set of its neighbors, $E(i)$ and $B(i)$ be the energy and the number of neighbors of the ith neighbor respectively, $i \in \mathcal{N}$. The thresholds are set as the linear combination of the maximum and mean value of corresponding parameters as in (3.27) and (3.28) so that the thresholds are adapted to the current distribution of parameters and take values between the maximum and mean.

$$E_{Th} \triangleq \gamma_1 \max_{i \in \mathcal{N}} E(i) + (1-\gamma_1) \operatorname{mean}_{i \in \mathcal{N}} E(i) \tag{3.27}$$

$$B_{Th} \triangleq \gamma_2 \max_{i \in \mathcal{N}} B(i) + (1-\gamma_2) \operatorname{mean}_{i \in \mathcal{N}} B(i) \tag{3.28}$$

The conditions can be relaxed by decreasing γ_1, γ_2, where $\gamma_1, \gamma_2 \in [0, 1]$. Since there is no closed-form objective function, it is difficult to determine optimal γ_1, γ_2 analytically. Fortunately, our experiments show that the performance is not sensitive to the setting of γ_1, γ_2. Thus, we simply choose a smaller value for γ_1 and a larger value for γ_2 as $\gamma_1 = 0$, $\gamma_2 = 0.8$, because we want to emphasize the position condition in order to achieve energy efficiency and relax the energy condition in order to accept more nodes into the headship auction.

Depending on their conditions, the nodes classify themselves into three categories shown in Fig. 3.4. Note that $DIFS_B = DIFS_A + CW_{min}$ in Fig.3.5, Category-B bidders have to wait longer than Category-A to ascertain there are no Category-A bidders in their neighborhoods. The extreme case that no heads are elected is avoided by permitting Category-B bidders into the headship auction because it is impossible that there are only Category-C nodes in the neighborhood.

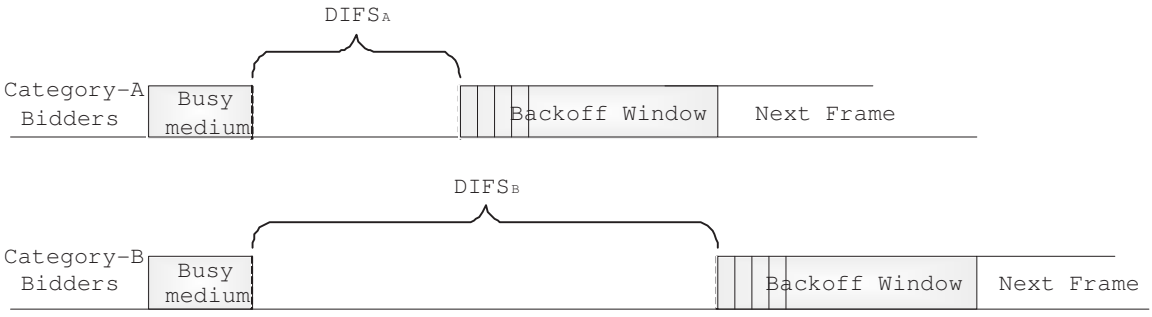

Figure 3.5. The Medium Access Control used in MCCHA.

Once a node successfully sends out the "headship claim", its neighbors must join it by sending "Request to join". Since these requests can be eavesdropped by their neighbors, their neighbors can correspondingly correct their numbers of unclustered neighbors. If a node finds all its neighbors are clustered, it can elect to be a cluster head by sending out a "headship claim". Those nodes outside the neighborhood of existing cluster heads cannot join any clusters. When the public channel is idle again, which indicates there

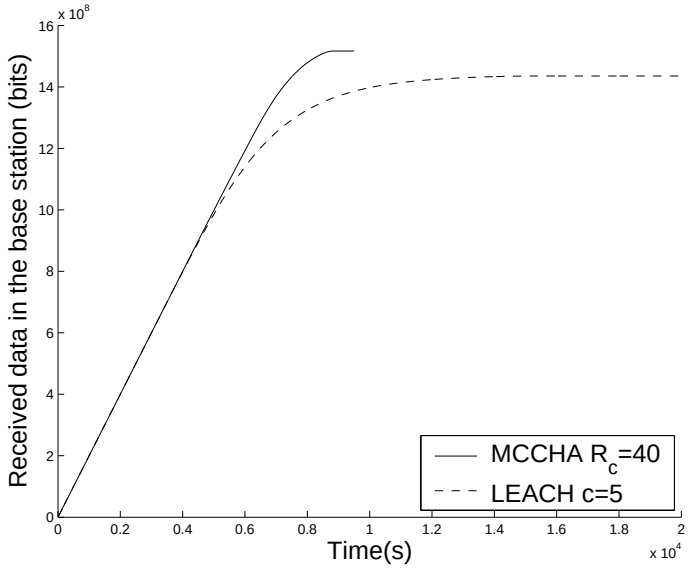

(a)

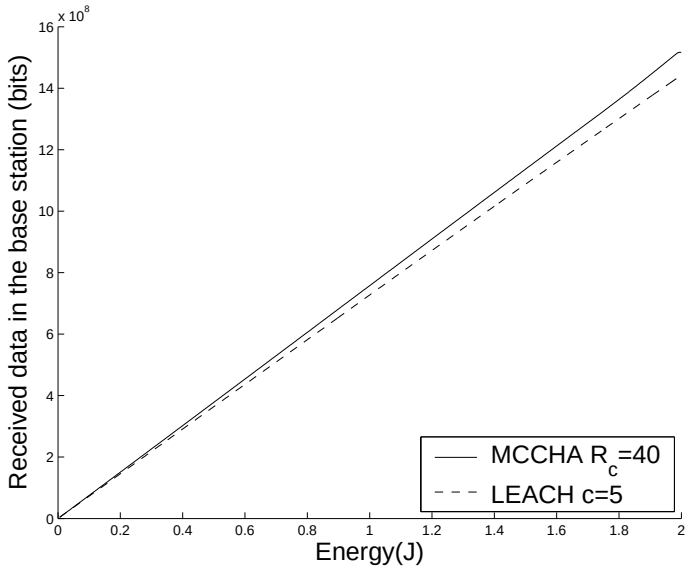

(b)

Figure 3.6. MCCHA vs. LEACH. (a) Amount of data received at the base station over time. (b) Amount of data received at the base station per given amount of energy.

is no node in its neighborhood trying to join existing clusters, another round of auction will begin until all nodes are clustered.

3.3 Simulations

In this section, we compare the performance of MCCHA and LEACH using computer simulations. 100 nodes with 2J initial energy were evenly distributed in a circular

region with diameter $100m$, and the base station was located at $(125m, 0)$. The data generating rate at each nodes is We ran LEACH and MCCHA over 1000 random network topologies for each c or R_c and took average of collected data.

3.3.1 MCCHA vs. LEACH

In this case, MCCHA is compared to native LEACH for nearly perfect data correlation ($\alpha = 0.001$). Our results show that the *maximum transportation*, the total data delivered back to the base station during a simulation, was maximized at $c \approx 7$ for LEACH and $R_c \approx 40m$ for MCCHA (See Table 3.1 and 3.2).

Table 3.1. Data of LEACH.

c	Effective Lifetime (s)	Maximum Transportation (bits)	Average DER (bit/J)	std DER
1	2400	8.9245e+008	5.7636e+006	1.9715e+006
3	4480	1.3304e+009	5.6989e+006	2.3275e+006
5	5200	1.4356e+009	5.8298e+006	2.5481e+006
7	5320	1.4169e+009	6.0806e+006	2.3895e+006
9	5240	1.3729e+009	6.1368e+006	2.2529e+006

Table 3.2. Data of MCCHA at $\alpha = 0.001$.

R_c (m)	Effective Lifetime (s)	Maximum Transportation (bits)	Average DER (bits/J)	std DER
10	7440	1.0256e+009	5.2086e+006	2.1247e+006
30	8560	1.4689e+009	7.1239e+006	1.5987e+006
40	8460	1.5169e+009	7.2989e+006	1.5862e+006
50	7200	1.5095e+009	7.2167e+006	1.5846e+006
80	4980	1.4077e+009	6.4853e+006	1.8423e+006

At first glance, LEACH seems have longer lifetime than MCCHA as shown in Fig.3.6(a). However, a further study of Fig.3.8 reveals that LEACH cannot guarantee the

data delivery during the later phase. The reason is that the ill result of random election (e.g. too few heads are elected) often puts tremendous burden on the heads whose energy is already low during the later phase. After the heads are exhausted quickly, the cluster members remain idle during the rest of that round, which seems to extend the lifetime. Therefore, we define the effective lifetime as when the data loss remains below 10 percent. Fig.3.8 shows that MCCHA extends the effective lifetime by about 3200s.

Another good measurement of energy efficiency is the ratio of data transportation over energy consumption, termed as Data/Energy Ratio(DER), which is indicated by the slope in Fig.3.6(b). Higher slope implies the corresponding scheme can transport more data with given amount of energy dissipation. Fig.3.6(b) shows MCCHA increased DER by about 25%. The analysis in section 3.1.3 indicates that R_c should be adapted to the

Table 3.3. Data of MCCHA at $\alpha = 0.05$.

R_c (m)	Effective Lifetime (s)	Maximum Transportation (bits)	Average DER (bits/J)	std DER
5	5940	7.1606e+008	3.9839e+006	2.0786e+006
10	6080	7.738e+008	4.1198e+006	1.8566e+006
15	5660	7.5131e+008	3.9482e+006	1.7069e+006
20	5260	7.0965e+008	3.6612e+006	1.645e+006
40	4220	5.8698e+008	3.0171e+006	1.4857e+006

decreasing node density. Since the death of nodes decreases the node density, we expect the optimal R_c to decrease accordingly. However, since MCCHA remarkably extends the effective lifetime, the number of survival nodes does not decrease visibly during most of the network lifetime. Therefore, we need not adapt R_c to keep energy efficiency.

3.3.2 Optimal R_c at Varying Data Aggregation Effect

In this case, MCCHA is evaluated at different α. We ran 1000 simulations at different R_c with $\alpha = 0.05$ to determine optimal R_c. Table 3.3 shows that the performance

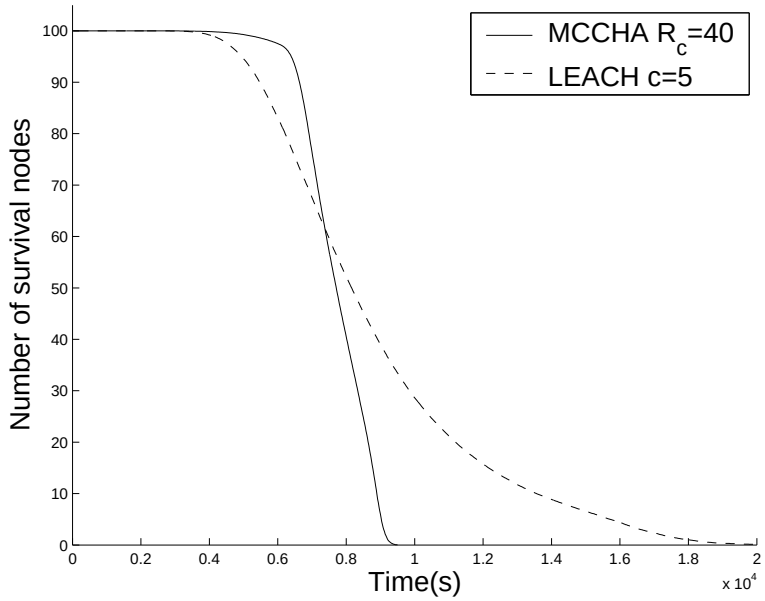

(a)

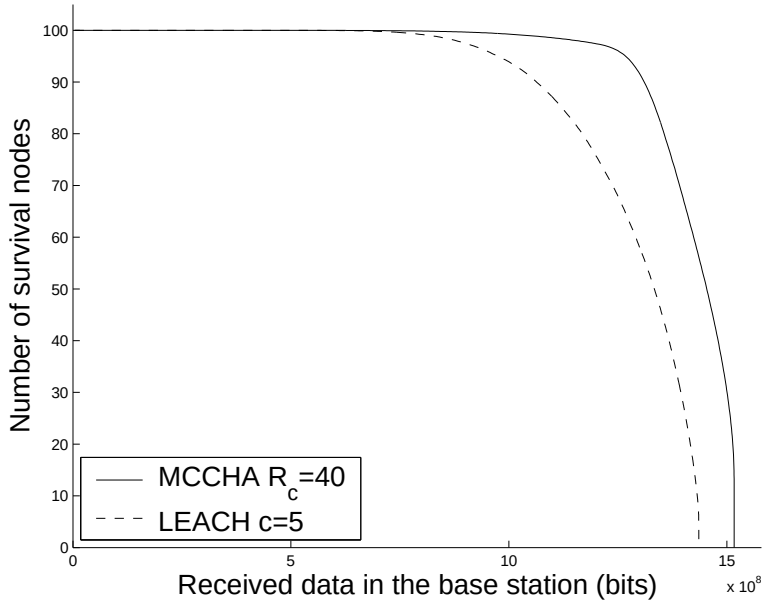

(b)

Figure 3.7. MCCHA vs. LEACH. (a) Number of survival nodes over time. (b) Number of survival nodes per amount of data received in the base station.

of MCCHA is optimal at around $R_c = 10m$, which is far from $R_c = 40m$ with $\alpha = 0.001$. The reason that the smaller clusters are formed is that the influence range shrinks when the data correlation decreases. These values of R_c agree well with the analysis in section 3.1.3 for both values of α. This shows the advantage of MCCHA over original LEACH; the clusters resulting from MCCHA conform to the energy-efficient expectation. This

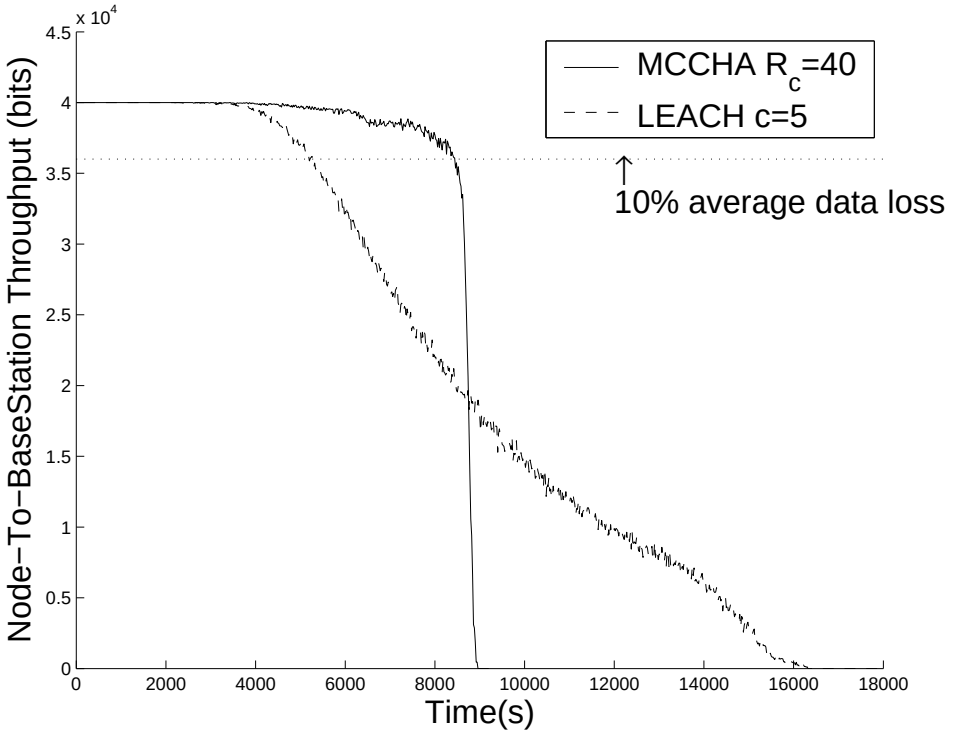

Figure 3.8. MCCHA vs. LEACH. Node-to-basestation throughput over time.

also shows the advantage of our data correlation model; we can easily fit the simulation scenarios for the phenomena of interest by varying α.

3.4 Conclusion

The previous clustering researches often take a global approach, which is appropriate for global optimization. However, when a distributed clustering is desired, the already-answered questions such as "How many clusters should the nodes be partitioned into?" have to be translated into a distributed version, that is, ''What's the appropriate cluster size?", because it is easier for a node to know its cluster size than the number of clusters in the whole network. In this paper, we take a fully distributed approach to energy efficiency for WSN. Motivated by the local energy efficiency criterion, we propose using the cluster size instead of the number of clusters as the clustering objective parameter in clustering. Furthermore, we utilize the medium contention to implement the headship auction to keep the cluster size within an ideal range. As shown by the

simulations, although the proposed MCCHA uses only local information, it achieves better energy efficiency than native LEACH in terms of Data/Energy Ratio and effective lifetime. The simulations also show that the optimal cluster radius obtained from the experiments agrees well with the analysis of optimal clustering, which indicates the performance of our distributed clustering is close to that of the global optimal one [91].

CHAPTER 4

CLUSTERING IN UNDERWATER SENSOR NETWORKS

4.1 Optimal Clustering

In this section, we analyze the energy consumption in UW-ASN and then study the relationship between cluster size and energy saving [92].

4.1.1 Problem Formulation

Clustering has been widely used in pattern recognition, and we use it to obtain the energy-efficient organization for UW-ASN. Consider a heterogeneous UW-ASN, in which the low-capacity sensors serves as cluster members and are randomly distributed, and the high-capacity sensors serve as cluster heads and are manually positioned. If we determine the optimal cluster size, then the required number of high-capacity sensors and their ideal positions can also be determined. In the following discussion, we assume the underwater sensor nodes can determine the distance between them via ultrasonic ranging or other techniques [93, 94].

For each bit sent from lower-capacity nodes, the energy consumption at the ith member of the kth cluster for each bit of data is

$$E_{CM(ki)} = E_{elec} + T_b C H r_{ki} e^{a(f) r_{ki}} \tag{4.1}$$

where r_{ki} is the distance from the kth cluster head and its ith member. The cluster head receives collects all the data from its member and then perform data aggregation. On the average, only η bit remains for each incoming bit and η is also referred to as data aggregation ratio. Because the MCUs (Microprogrammed Control Unit) used in underwater sensors often work at much lower power than the hydrophones, the energy

consumed in data procession is ignored here [95]. Similarly, the energy consumption of the kth high-capacity node is

$$E_{CH(k)} = N_k E_{elec} + N_k \eta (E_{elec} + T_b CH d_k e^{a(f)d_k}), \tag{4.2}$$

where N_k is the number of low-capacity nodes in the kth cluster and $\sum_{k=1}^{c} N_k = N$, d_k is the distance from the kth cluster head to the surface sink.

Considering all c clusters, the overall cost is

$$E_{total} = \sum_{k=1}^{c} (E_{CH(k)} + \sum_{i=1}^{N_k} E_{CM(ki)}). \tag{4.3}$$

Taking the expected value of the overall energy cost, we obtain $\bar{E_{total}}$ as the objective function.

$$\begin{aligned} \bar{E}_{total} &= k\bar{E}_{CH} + N\bar{E}_{CM} \\ &= NE_{elec} + NT_b CHE[re^{a(f)r}] \\ &+ NE_{elec} + N\eta(E_{elec} + T_b CHE[de^{a(f)d}]) \end{aligned} \tag{4.4}$$

Obviously, the determining factor is $E[re^{a(f)r}]$ and $E[de^{a(f)d}]$, thus, we rewrite (4.4) as

$$\begin{aligned} \bar{E}_{total} &= 2NE_{elec} + NT_b CHJ_{CM} \\ &+ N\eta(E_{elec} + T_b CHJ_{CH}) \end{aligned} \tag{4.5}$$

$$J_{CM} = E[re^{a(f)r}], \tag{4.6}$$

$$J_{CH} = E[de^{a(f)d}],$$

Suppose the frequency allocation is irrelevant to r, which is the case for most applications in use, $\alpha(f)$ and r are independent.The best cluster size could vary for difference deployments. In the following subsection, we will discuss several typical scenarios.

4.1.2 Solution for Random Deployment

Suppose the low-capacity sensors are deployed at random, then their locations would follow the two-dimension Poisson distribution, i.e., the number of nodes N_A in area A is given by,

$$Pr(N_A) = (\lambda A)^{N_A} e^{-\lambda A} / N_A!, \tag{4.7}$$

where λ is the node density. A useful property of the Poisson process is that *if the number of nodes occurring in the area A is N, then the individual outcomes of N nodes are distributed independently and uniformly in the area A.* For the single-hop cluster, in which all cluster members can communicate with the cluster head directly, the distance r from a cluster member to the cluster head has the cdf given by

$$F(r) = \frac{\pi r^2}{\pi R_c^2}, \tag{4.8}$$

where R_c is the cluster size. Thus the pdf of r is

$$f(r) = \frac{2r}{R_c^2}. \tag{4.9}$$

$$\begin{aligned} J_{CM} &= \int_0^{R_c} r e^{a(f)r} \frac{2r}{R_c^2} dr \\ &= \frac{2}{R_c^2}[\frac{e^{a(f)r}}{a(f)^3}(a(f)^2 r^2 - 2a(f)r + 2)]_0^{R_c} \\ &= \frac{2e^{a(f)R_c}}{a(f)^3}(a(f)^2 - \frac{2a(f)}{R_c} + \frac{2}{R_c^2}) - \frac{4}{a(f)^3 R_c^2} \end{aligned} \tag{4.10}$$

Similarly, the cluster heads should also be evenly distributed in the area of interest. Suppose the area of interest is circular with radius R, then desirable location of cluster heads is depicted by the shadow in Fig.4.1.

$$\begin{aligned} J_{CH} &= \int_0^{R-R_c} r e^{a(f)r} \frac{2r}{R^2} dr \\ &= \frac{2}{R^2}[\frac{e^{a(f)r}}{a(f)^3}(a(f)^2 r^2 - 2a(f)r + 2)]_0^{R-R_c} \\ &= \frac{2e^{a(f)(R-R_c)}}{a(f)^3 R^2}(a(f)^2(R-R_c)^2 - 2a(f)(R-R_c) \\ &\quad +2) - \frac{4}{a(f)^3 R^2} \end{aligned} \tag{4.11}$$

By setting the derivative of (4.10) to zero, we obtain

$$\begin{aligned} \frac{\partial \bar{E}_{total}}{\partial R_c} = &\frac{8 + 2e^{aR_c}(-4 + 4aR_c - 2a^2 R_c^2 + a^3 R_c^3)}{a^3 R_c^3} \\ &+\eta(\frac{1}{a^3 R^2}(e^{-aR_c}(-4ae^{aR_c} + 2e^{aR} \end{aligned}$$

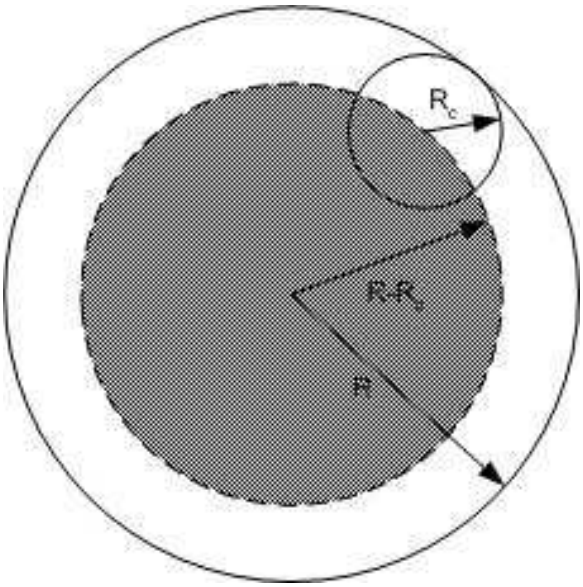

Figure 4.1. Footprint of cluster heads.

$$(a^2R_c + a(2 - 2aR + aR_c)))) -$$
$$\frac{1}{a^2R^2}(e^{-aR_c}(-4e^{aR_c} +$$
$$2e^{aR}(2 + aR(-2 + aR) +$$
$$aR_c(2 - 2aR + aR_c))))) = 0 \quad (4.12)$$

The solution can be obtained numerically. The second-order derivative of (4.10) is given by

$$\begin{aligned}
\frac{\partial^2 \bar{E}_{total}}{\partial R_c^2} &= \frac{6(-4 + 2e^{aR_c}(2 + aR_c(-2 + aR_c)))}{a^3R_c^4} - \frac{1}{a^3R_c^3}(4(2e^{aR_c}(a^2R_c + a(-2 + aR_c)) \\
&+ 2ae^{aR_c}(2 + aR_c(-2 + aR_c)))) + \frac{1}{a^3R_c^2}(4a^2e^{aR_c} + 4ae^{aR_c}(a^2R_c + a(-2 + aR_c)) \\
&+ 2a^2e^{aR_c}(2 + aR_c(-2 + aR_c))) + \eta(\frac{e^{-aR_c}(4a^2e^{aR} - 4a^2e^{aR_c})}{a^3R^2} \\
&- \frac{1}{a^2R^2}(2e^{-aR_c}(-4ae^{aR_c} + 2e^{aR}(a^2R_c + a(2 - 2aR + aR_c)))) \\
&+ \frac{1}{aR^2}(e^{-aR_c}(-4e^{aR_c} + 2e^{aR}(2 + aR(-2 + aR) \\
&+ aR_c(2 - 2aR + aR_c))))) \quad (4.13)
\end{aligned}$$

Substitute (4.12) into (4.13), it can be shown

$$\frac{\partial^2 \bar{E}_{total}}{\partial R_c^2} > 0, \quad (4.14)$$

which shows $\bar{E}_{total}$ is minimized at the solution of (4.12).

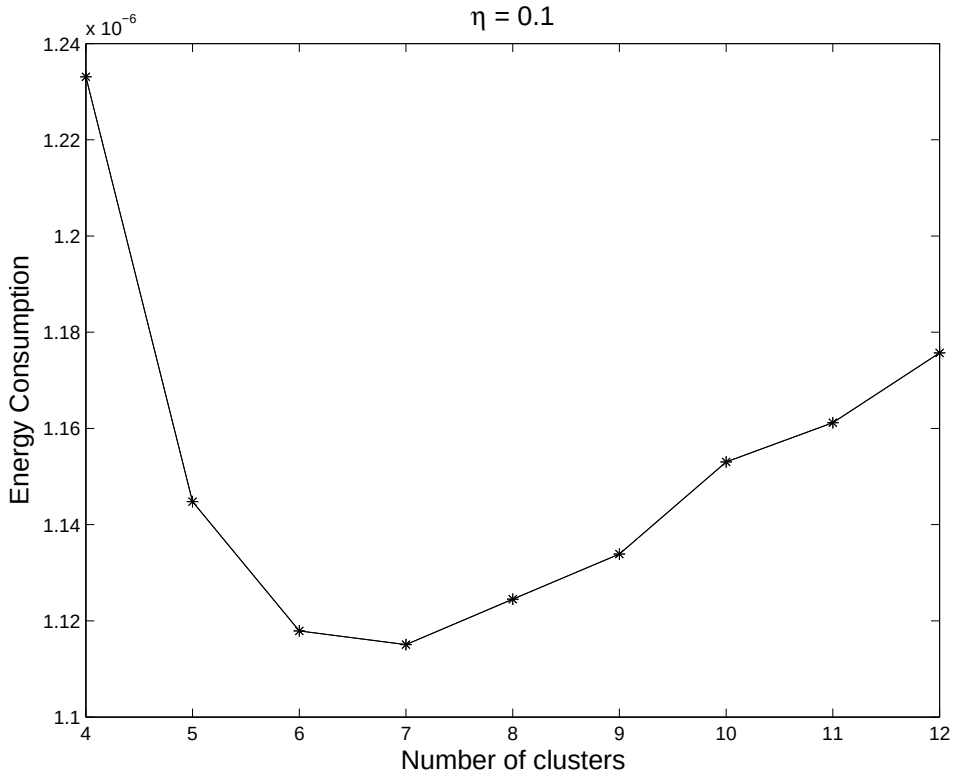

Figure 4.2. E_{total} vs. the number of clusters.

4.2 Simulations

In this section, we validate our optimum cluster size analysis using computer simulations. $N = 100$ nodes were uniformly distributed in a circular region with diameter $1000m$ and the water depth was $10m$. The surface sink was set at the center. For a given number of clusters, we used Fuzzy-C-Means(FCM) to form the clusters and then measured the energy consumption of the clustered network. We ran 100 simulations on randomly generated network topologies and took average of collected data.

Fig.4.2, Fig.4.3 and Fig.4.4 show the energy consumption for the given number of cluster with data aggregation ratio η =0.1, 0.5 and 1.0, respectively. The plotted data show concave curves, which indicates there does exists a optimal cluster size at which

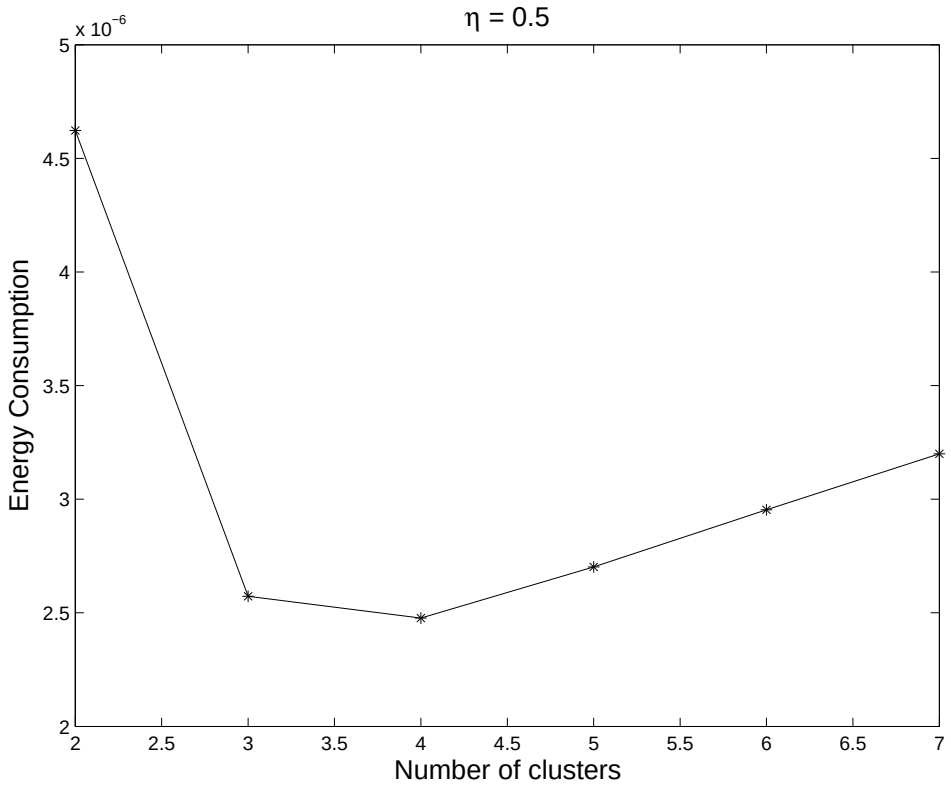

Figure 4.3. E_{total} vs. the number of clusters.

Table 4.1. Calculated number of clusters.

η	R_c	k
0.1	191.7	6.8
0.5	263.5	3.6
1	293.6	2.9

the energy consumption is minimized. We also solve (4.12) numerically, and translate the cluster radius into the number of clusters according to

$$k = \frac{\pi R^2}{\pi R_c^2}. \tag{4.15}$$

The calculated k's are listed in Table 4.1. Compared to Table 4.1, the figures 4.2, 4.3 and 4.4 show that the energy consumption minimum does occurred around the calculated number of clusters, proving our numerical analysis matches well with the simulation results.

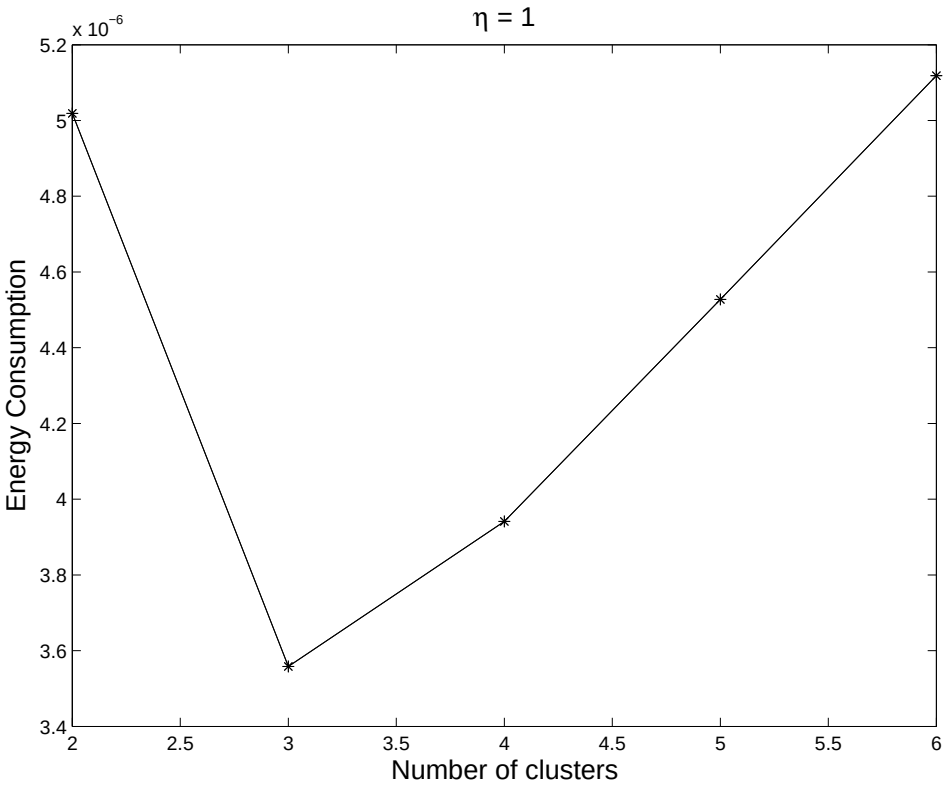

Figure 4.4. E_{total} vs. the number of clusters.

4.3 Conclusion

Although clustering has been well studied for the terrestrial WSN, the unique characteristics of the underwater acoustic communications call for a new study. Because the path loss is not only relevant to the distance, but also related to the working frequency, the optimal cluster size for UW-ASN shows different properties from the terrestrial WSN. In addition, the data aggregation also play an important role in determining the optimal cluster size. The simulation results agrees well with our numerical analysis [96].

CHAPTER 5

MODELING HOP-DISTANCE RELATION

5.1 Probabilistic study

In this chapter, we model the end-to-end distance for given number of hops and then apply our model to ranging problem [97].

5.1.1 Problem Formulation

We assume a general beacon scenario, in which anchors sends out beacon packets informing other nodes about their locations. These beacon packets are also relayed so that nodes outside the anchors' transmission range could also received the beacons. Suppose the sensor nodes are placed on a plane at random at an average density of λ nodes per square meters. Nonetheless, clarifications about several terms are necessary, because they have been used in a wide variety of senses [98–102].

Firstly, our study on end-to-end distance for given number of hops is based on local coordinate system, which could be translated into a global coordinate system if enough nodes in the local coordinate system have known global coordinates. In previous research, anchors refer to beacons, whose locations are known and broadcast to other nodes. However, in our study, an anchor is simply a specific node used in establishing the local coordinate system. An anchor could have global coordinates or not, which is of no interest to our study. Therefore, our study is applicable to both anchor-based and anchor-free approaches.

Secondly, we assume the beacon packets are distributed in an ad hoc fashion. Although better routing, such as geographic routing [82, 103–108], are proposed for WSN, they are not suitable for relaying beacon packets, because during this phase, most nodes have no knowledge about locations of their own and neighbors'. Under such circumstances, we have to assume the beacon packets are simply flooded throughout the sensor

network, except that nodes can only relay the beacon packets incoming with least number of hops and discard those via more hops.

Let $N(A)$ be the number of nodes in area A, it can be shown that $N(A)$ is a two-dimensional Poisson point process with density λ [109]. One property of the Poisson process is that *if the number of nodes occurring in the area A is N, then the individual outcomes are distributed independently and uniformly in the area A.* That is, if N nodes are placed at random in the area A, then the probability of a specific node in the subarea B is B/A, given $B \in A$.

Table 5.1. Definition of Variables

Variable	Definition
$\vec{r} = (r, \theta)$	the polar coordinates of a node
t_i	the distance from the $(i-1)$-hop node to the i-hop node
H_i	the event "the specific node is within i hops, but beyond $(i-1)$ hops from the source."

Assume the area A is large enough so that none of the anchor nodes is near the border and the transmission range is R. The problem of interest is to find the distance from a specific node to the anchor given this node is within i hops from the anchor. The definitions of variables are listed in Table 5.1. Note that the event H_i can also be described as "the minimum number of hops from the anchor to the specific node is i".

5.1.2 Single-Hop Case

Consider the first hop case shown in Fig.5.1, the conditional cdf can be expressed by

$$P[r_1 < r|H_1] = P[r_1 < r|r_1 < R] = \frac{r^2}{R^2} \tag{5.1}$$

Taking derivative,

$$f_{(r_1|H_1)}(r) = \frac{2r}{R^2} \tag{5.2}$$

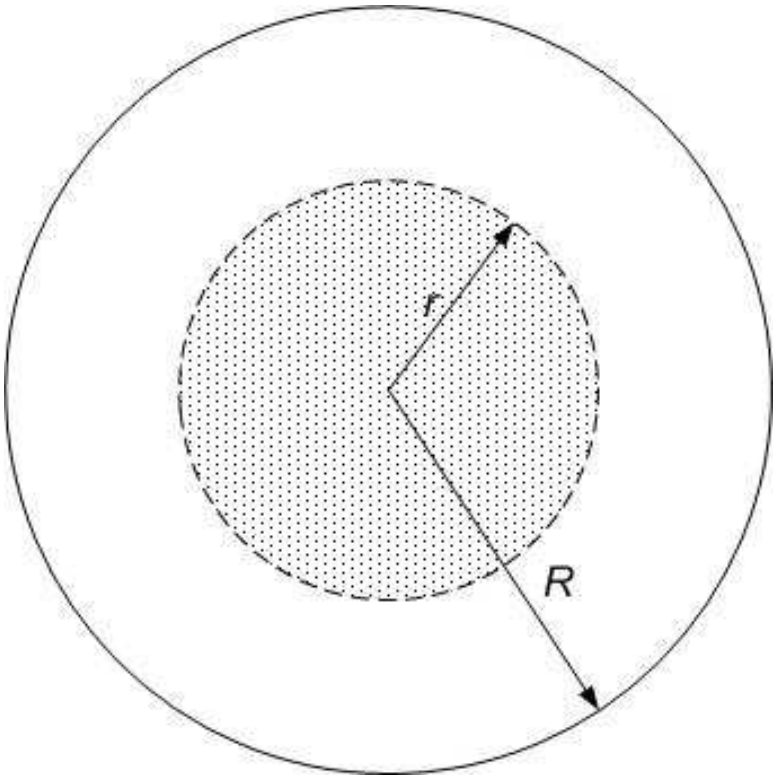

Figure 5.1. The single-hop case.

And the conditional mean and variance are $2R/3$ and $R^2/18$, respectively, which are solely determined by the transmission range R and irrelevant to the node distribution density λ. This is due to the uniform node distribution; no matter how large the density could be, it would not give any bias to the conditional mean and variance.

5.1.3 Two-Hop Case

Conditional on the value of r_1, the cdf for t_2 is

$$F_{t_2|r_1|H_2}(t_2) = \frac{B}{\pi R^2}, \tag{5.3}$$

where B is the area of the region inside the circle of center $\vec{r}_1$ but outside the circle of center $\vec{r}_0$. B is equal to

$$\pi(t_2)^2 - (t_1)^2(\phi_1 - \frac{1}{2}\sin 2\phi_1) - (t_2)^2(\phi_2 - \frac{1}{2}\sin 2\phi_2), \tag{5.4}$$

where

$$\phi_1 = \cos^{-1}(1 - \frac{(t_2)^2}{2(t_1)^2}), \tag{5.5}$$

$$\phi_2 = \cos^{-1}(\frac{t_2}{2t_1}). \tag{5.6}$$

The conditional pdf of t_2 is obtained by taking the derivative of (5.3).

$$f_{t_2|r_1|H_2}(r) = \frac{d}{dt}\frac{B}{\pi R^2}, \tag{5.7}$$

By taking expected value of (5.7),

$$f_{t_2|H_2}(t) = \int_0^R f_{r_1}(s)\frac{d}{dt_2}\frac{B}{\pi R^2}ds, \tag{5.8}$$

r_2 is determined by

$$r_2 = \sqrt{(t_1)^2 + (t_2)^2 - 2t_1t_2\cos\phi}, \tag{5.9}$$

where ϕ is the angle between t_1 and t_2 and uniformly distributed in $[-\phi_2, \phi_2]$. Although it is possible to derive the pdf of r_2 from (5.9), it is awkward to evaluate explicitly. Furthermore, note that r_n depends on r_{n-1}, a nested integral as in (5.10) is generally required for such evaluations. Thus, for the end-to-end distance for two and more hops, we will postulate their distribution from the collected simulation data in the next section.

$$\begin{aligned} p(r_n|H) = & \int_R^{(n-1)R} \int_R^{(n-2)R} \cdots \int_0^R p(r_n|r_1, r_2, \cdots, r_n - 1, H) \\ & f(r_{n-1}|r_1, r_2, \cdots, r_{s-2}, H) \cdots \\ & f(r_1|H)dr_1 \cdots dr_{n-2}dr_{n-1} \end{aligned} \tag{5.10}$$

5.2 Statistical Analysis

All the simulation data are collected from such a scenario that N sensor nodes were uniformly distributed in a circular region of radius of 300 meters. For convenience, polar coordinates were used. The anchor node was placed at $(0, 0)$. We ran simulations

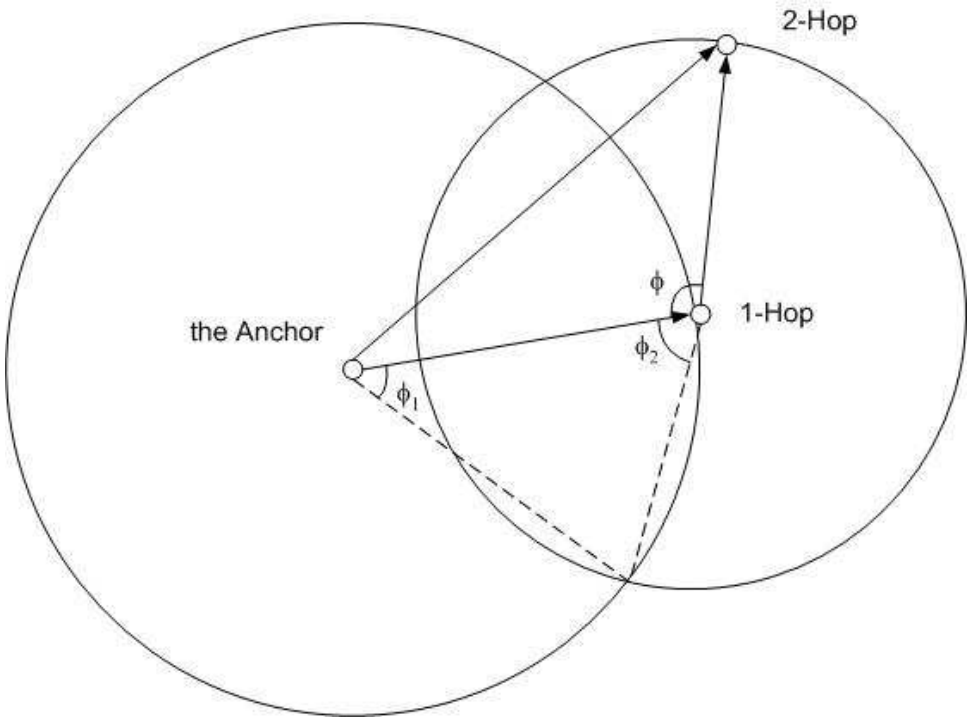

Figure 5.2. Two hops.

for extensive settings of node density λ and transmission range R. And for each setting of (N, R), we ran 300 simulations, in each of which all nodes are re-deployed from the beginning.

5.2.1 Single-Hop Distance

We plot the histogram of single-hop distance collected from simulations and compare with the theoretical result (5.2) in Fig. 5.3, which clearly shows that (5.2) fits the experimental data very well. Furthermore, a chi-square test was carried out to determine the goodness of fit of (5.2) to the experimental data.

The threshold for $30-1=29$ degrees of freedom at a 1% significance level is 49.59. Compared to this, $D^2 = 28.8728$ is well within the threshold. Thus, we establish that the data is in good agreement with (5.2).

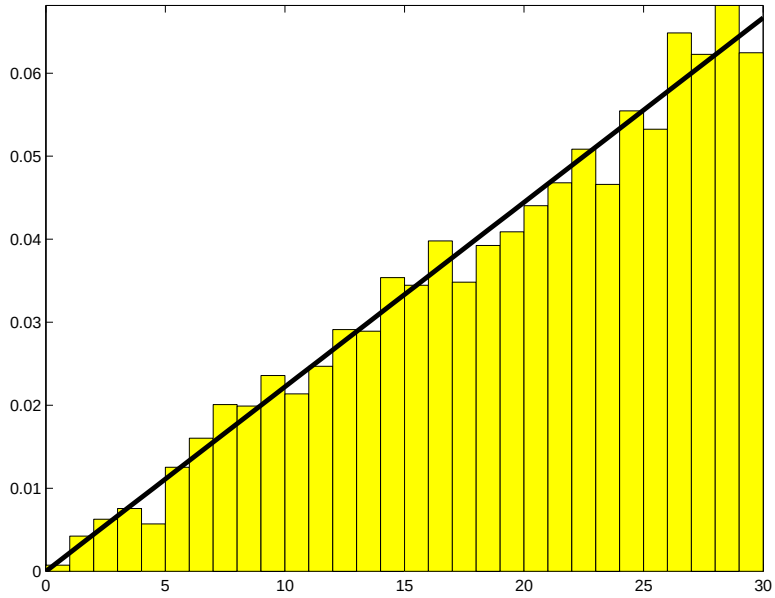

Figure 5.3. The histogram vs. postulated distribution for single-hop distance.

5.2.2 Two-Hop End-to-end Distance

Since there is no closed-form formula for the conditional pdf of end-to-end distance for two and more hops, we have to find a fit for it. We postulate the following pdf for the conditional pdf of two-hop end-to-end distance according to the experimental data plotted in Fig. 5.4, whose characteristic curve clearly shows a Beta distribution shape. The general pdf of Beta distribution is

$$f_X(x) = C(x-a)^{p-1}(b-x)^{q-1}, \tag{5.11}$$

where p and q are the shape parameters, a and b are the lower and upper bounds, and C is a numerical factor to make the complete probability one. The bounds a and b can be easily determined as $a = 0$ and $b = 2R$. Since the maximum of (5.11) occurs at $b(p-1)/(p-1+q-1)$, which is at $3R/2$ in Fig. 5.4, therefore, $p = 4$ and $q = 2$ would be a good guess. The remaining parameter C is determined by

$$C = \int_R^{2R} \frac{(2R-s)s^3}{\mathcal{B}(4,2)(2R)^5}. \tag{5.12}$$

The postulated Beta distribution and histogram are drawn together in Fig. 5.4, which clearly shows a close match.

Figure 5.4. The histogram vs. postulated distribution for two-hop distance.

5.2.3 Three-And-More-Hop End-to-end Distance

When the number of hops increases beyond three, the end-to-end distance distribution approaches Gaussian (See Fig. 5.5, Fig.5.6, Fig.5.7 and Fig.5.8). For a more formal analysis about its Gaussianity, we list their skewness and kurtosis in Table 6.1. Note that both skewness and kurtosis are well within tolerance, we postulate Gaussian distribution for three-and-more-hop end-to-end distance. The mean and std can be estimated from the experimental data (see Table 6.1). We plot the postulated Gaussian distribution and histogram together in Fig. 5.5, Fig.5.6, Fig.5.7 and Fig.5.8, which clearly show a close match for each case.

5.2.4 Optimum Estimation and Error Analysis

Once the condition pdf is known, the distance estimation is straightforward. The optimum unbiased estimator is $E[r_n|H_n]$, and accordingly, the RMSE can be minimized to $\sqrt{VAR[r_n|H_n]}$. In APS/Hop-TERRAIN, the distance is assumed to increase linearly

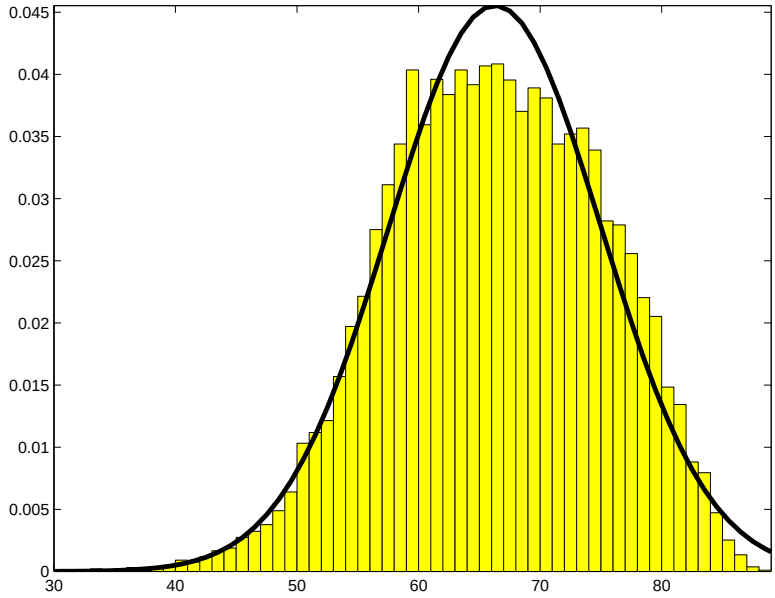

Figure 5.5. The histogram vs. postulated distribution for three-hop distance.

with the number of hops, and thus, a linear estimator, $n*m1$, is used to estimate nth-hop distance. Accordingly, the MSE of the linear estimator is given by

$$\begin{aligned} MSE(H_n) &= E[(r_n - nm_1)^2] \\ &= VAR[r_n|H_n] + (m_n - nm_1)^2 \end{aligned} \tag{5.13}$$

The difference between the minimum RMSE and the biased RMSE given by APS/Hop-TERRAIN estimator is depicted in Fig.5.9, which increases drastically even when n is only moderately large. As discussed in the Introduction, there exists a lower bound of distance error for the RSS-based ranging technology. According to [52], the median localization error of commodity 802.11 technology is $10ft \approx 3.05m$. The RMSE we obtain in our simulations is around 8 meters, which is in the same order of magnitude as the distance error bound in [52]. Furthermore, in environment with irregular terrain, obstacles or other clutters, the shadowing effect may cause higher distance error. Since hop-based distance technology is immune to shadowing effect, it may outperform RSS-base ranging in these kinds of environment.

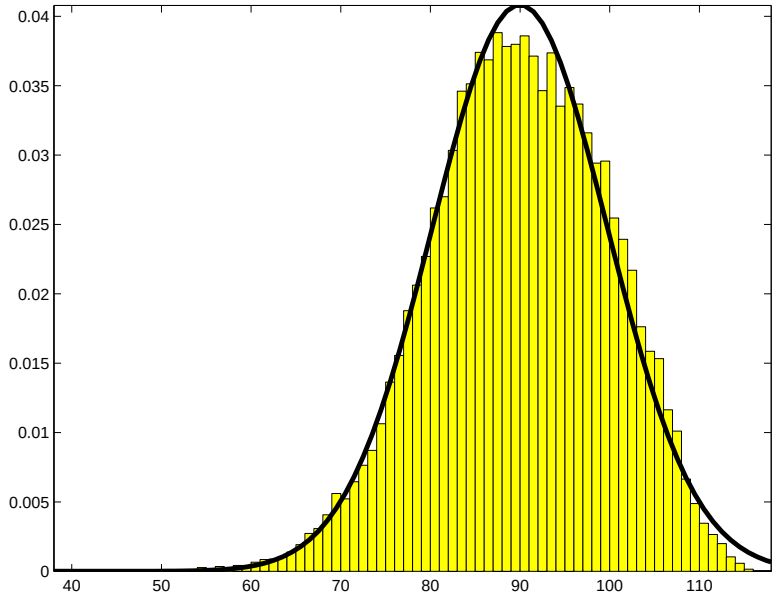

Figure 5.6. The histogram vs. postulated distribution for four-hop distance.

5.3 Conclusions

In this chapter, we study the modeling of the end-to-end distance for given number of hops in WSN. The experiments showed that the distance does not increase linearly with the number of hops. Therefore, the distance should be analyzed for each number of hops. We derived the distribution for single-hop distance and also showed that the complexity of derivation for multiple-hop distance is beyond practical interest. Thus, we postulate Beta distribution for two-hop end-to-end distance and Gaussian distribution for three-and-more-hop end-to-end distance. Computer simulations showed our postulated distributions agree well with the histograms. We also show that the distance error can be minimized by exploiting the distribution knowledge [110].

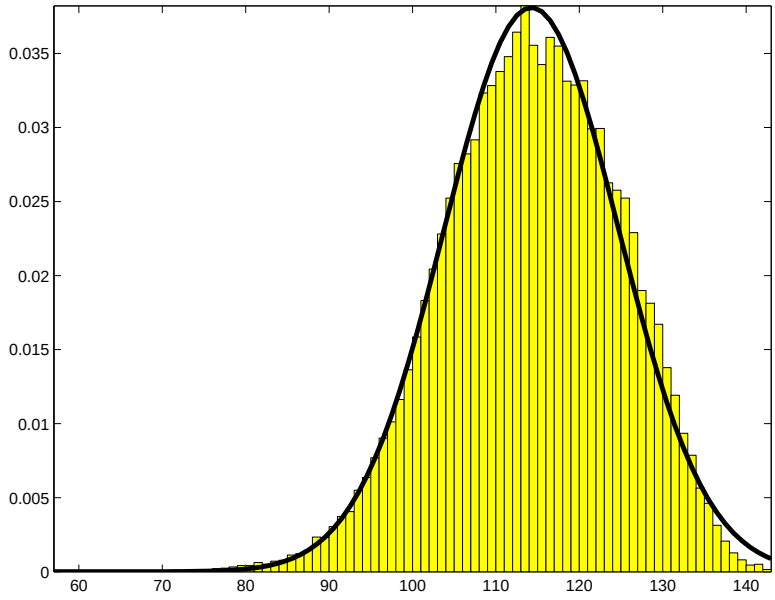

Figure 5.7. The histogram vs. postulated distribution for five-hop distance.

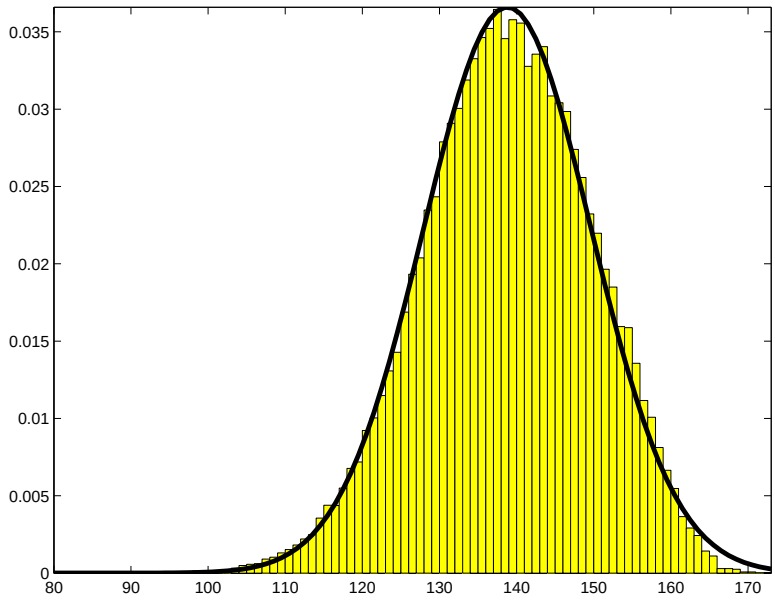

Figure 5.8. The histogram vs. postulated distribution for six-hop distance.

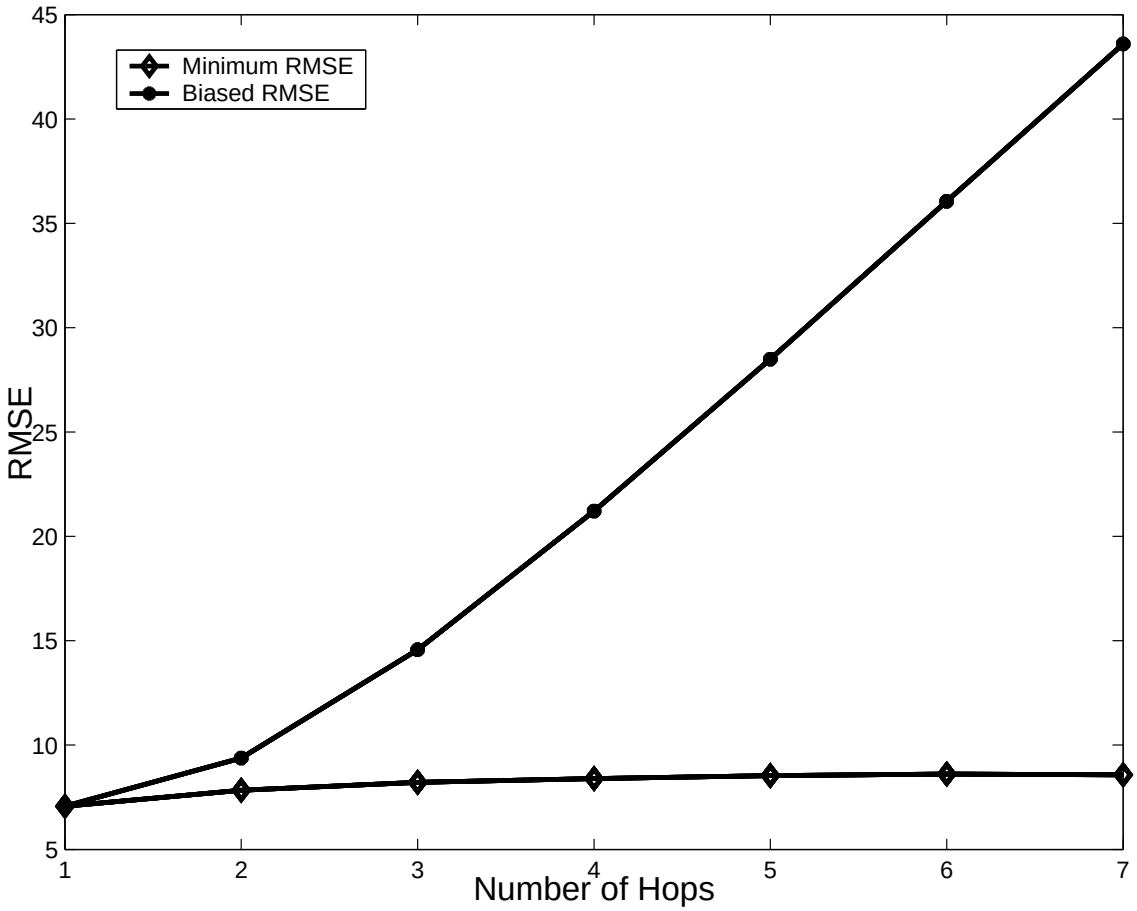

Figure 5.9. The RMSE bias vs. the number of hops. R=30m.

CHAPTER 6

HOP ESTIMATION GIVEN DISTANCE

6.1 Maximum Likelihood Analysis

Suppose the sensor nodes are placed on a plane at random at an average density of λ nodes per square meters. Let $N(A)$ be the number of nodes in area A, it can be shown that $N(A)$ is a two-dimensional Poisson point process with density λ. The problem of interest is to find the number of hops, denoted H_i needed to reach a specific destination r from a given source node. We can make a Maximum Likelihood (ML) decision,

$$\hat{H} = \arg\max f(r|H_i), i = 1, 2, 3, \cdots, \tag{6.1}$$

where H_i can also be described as "the minimum number of hops is i from the source to the specific node with Euclidean distance r". In the following discussion, we are trying to approximate $f(r|H_i)$ for 2-D Poisson distribution. Note that $r < R \rightarrow H_1$, we are more interested in multiple-hop distance relation, especially for i is relatively large.

6.1.1 Attenuated Gaussian Approximation

Table 6.1. Statistics of $f(r|H_i)$

Number of Hops	Mean	Std	Skewness	Kurtosis
1	19.991	7.0651	-0.57471	-0.58389
2	45.132	7.8365	-0.16958	-1.0763
3	72.01	8.2129	-0.10761	-1.0332
4	99.45	8.391	-0.07938	-0.97857
5	127.14	8.5323	-0.06445	-0.93104
6	154.96	8.6147	-0.05341	-0.9004
7	182.68	8.573	-0.07738	-0.91687

Since $f(r|H_i)$ is awkward to evaluate even using numerical methods, we use histograms collected from Monte Carlo simulations as substitute to the pdf. All the simulation data are collected from such a scenario that N sensor nodes were uniformly distributed in a circular region of radius of R_{Bound} meters. For convenience, polar coordinates were used. The source node was placed at $(0, 0)$. The transmission range was set as R meters. For each setting of (N, R_{Bound}, R), we ran 300 simulations, in each of which all nodes are re-deployed at random. We ran simulations for extensive settings of node

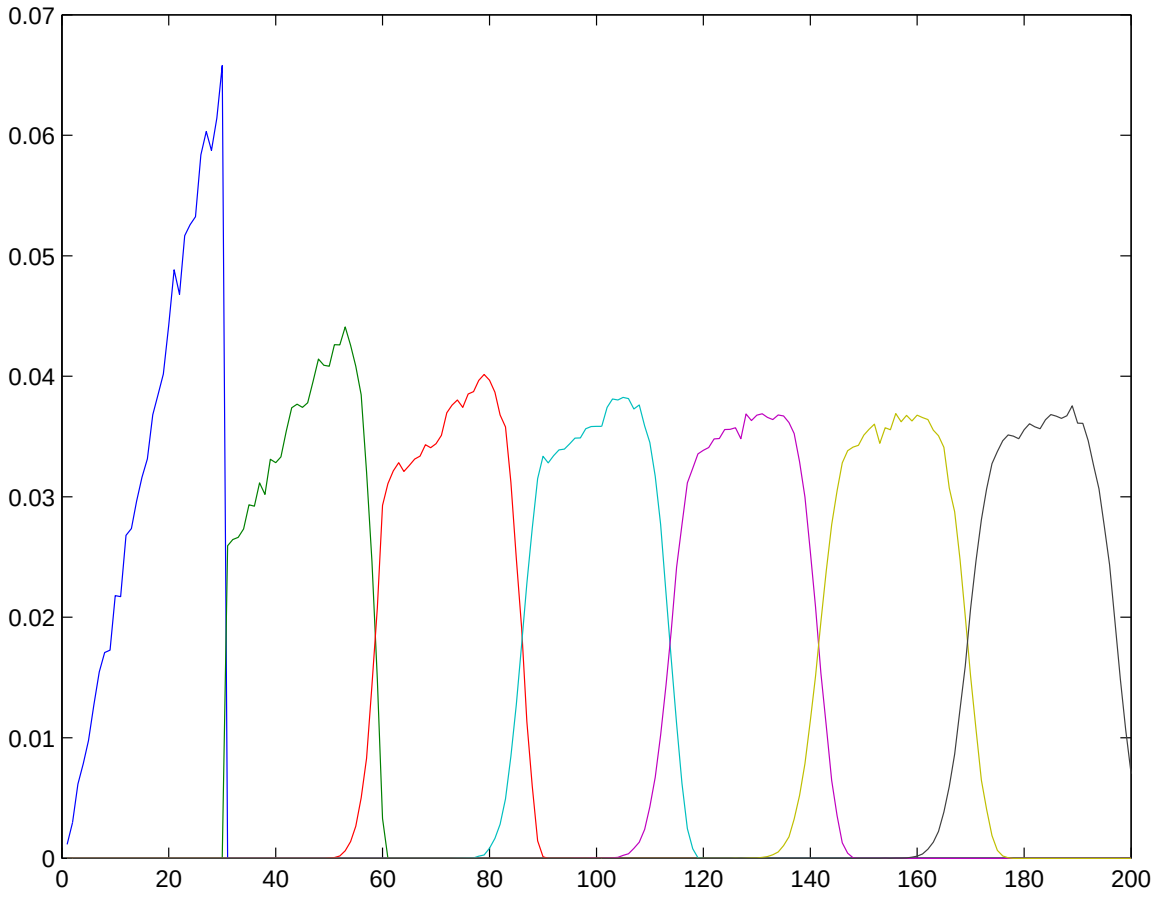

Figure 6.1. Histograms of hop-distance distribution. $(N = 1000, R_{Bound} = 200, R = 30)$.

density λ and transmission range R. Due to space constraints, only the histograms for $(N = 1000, R_{Bound} = 200, R = 30)$ are plotted in Fig. 6.1, which approximately shows that $f(r|H_i)$ approach the normal when H_i increases. Table 6.1 lists the first-, second-, third- and fourth-order statistics of $f(H, r)$. The statistics of seven-hop distance is

slightly aberrant because the 200 meter radius cuts off part of its range as shown in Fig.6.1. For $H_i = 3, 4, ..., 6$, the skewness is nearly zero and keeps decreasing. The same trend applies to kurtosis, though, its values is around -1, which shows the pdf's are not perfectly Gaussian. Furthermore, The postulated distribution and histogram are drawn together in Fig. 5.5, Fig. 5.6, Fig. 5.7 and Fig. 5.8, which clearly shows a close match for each case.

Thus, the objective function can be approximated by

$$\begin{aligned} f(r|H_i) &= \alpha^n \mathcal{N}(m_n, \sigma_n) \\ &= \frac{\alpha^n}{2\pi\sigma} e^{-\frac{(r-m_n)^2}{2\sigma_n^2}}, \end{aligned} \tag{6.2}$$

where α is the equivalent attenuation base, m_n and σ_n are the mean and standard deviation(std), respectively. The specific values of these parameters can be estimated from simulations. Our extensive simulations show that, even for only relatively large H_i, $f(r|H_i)$ has following properties,

1. $\sigma_n \approx \sigma_{n-1}$, which means the neighboring pdf's have similar spread.
2. $m_n - m_{n-1} \approx m_{n+1} - m_n$, which means the pdf's are evenly spaced.
3. $3 < \frac{m_n - m_{n-1}}{\sigma_n} < 5$, which means the overlap between the neighboring pdf's is small but not negligible. (As a rule of thumbs, $Q(3)$ is considered relatively small and $Q(5)$ is regarded negligible.)
4. $\frac{m_n - m_{n-2}}{\sigma_n} \gg 5$, which means the overlap between the non-neighboring pdf's is negligible.
5. $\alpha < 1$. For large density λ, $\alpha \to 1$. Along with Property 1, this tell us that the neighboring pdf's have nearly identical shape.

As shown in the following discussion, these properties largely simplify the decision rule and the error analysis. Another interesting observation, besides these properties, is that the following equations do not stand true.

$$m_n = nm_1 \tag{6.3}$$

$$m_n = nR \tag{6.4}$$

$$m_n = (n-1)R + R/2 \tag{6.5}$$

Although these equations sound plausible, they all give visible errors. The aforementioned estimator $[r/R]+1$ for H_i, though widely used, is not good in the new light shed by this study.

6.1.2 Decision Boundaries

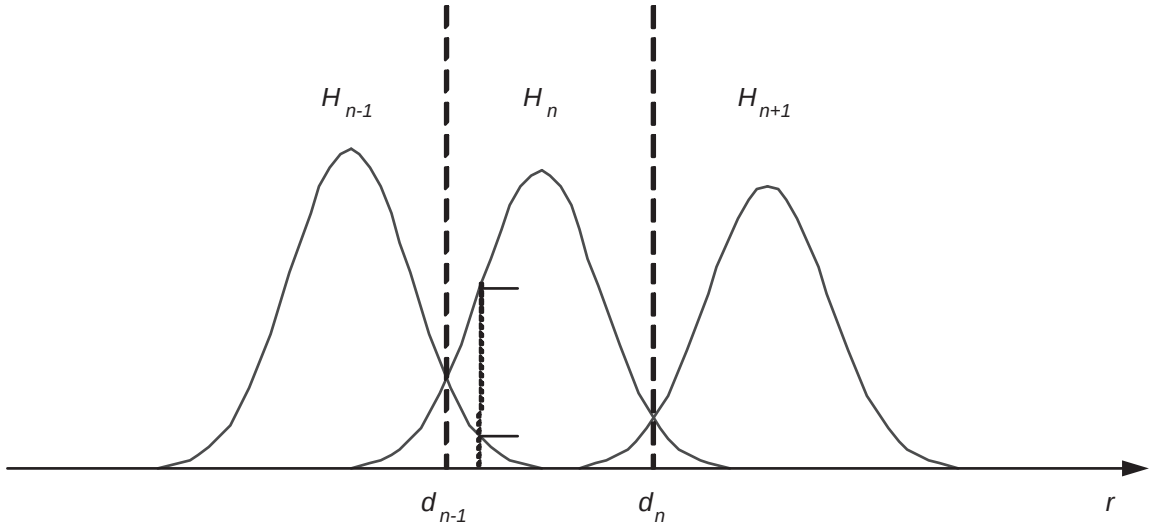

Figure 6.2. Gaussian Approximation.

Following (6.1), and observe the $f(r|H_i)$ in Fig. 6.2, the decision is needed only between neighboring H_i, that is,

$$f(r|H_n) \underset{n+1}{\overset{n}{\gtrless}} f(r|H_{n+1}). \tag{6.6}$$

This is because, for a specific value of r, there are only two values of H_i with dominating $f(r|H_i)$, compared to which $f(r|H_i)$ for other values of H_i is negligible. Substitute (6.2) into (6.6), we obtain the decision boundary d_n between the regions H_n and $H_n + 1$.

$$\begin{aligned} d_n &= \frac{B + \sqrt{B^2 + AC)}}{A} \\ A &= \sigma_{n+1}^2 - \sigma_n^2 \\ B &= m_n\sigma_{n+1}^2 - m_{n+1}\sigma_n^2 \end{aligned}$$

$$C = m_n^2\sigma_{n+1}^2 - m_{n+1}^2\sigma_n^2 + 2\sigma_n^2\sigma_{n+1}^2 \ln\alpha \tag{6.7}$$

Using Property 1,

$$d_n = \frac{m_{n+1}^2 - m_n^2 - 2\sigma_n^2 \ln\alpha}{2(m_{n+1} - m_n)} \tag{6.8}$$

For large density λ, Property 5 is applicable, (6.7) simplifies to

$$d_n = \frac{\sigma_n^2 m_{n+1} + \sigma_{n+1}^2 m_n}{\sigma_n^2 + \sigma_{n+1}^2} \tag{6.9}$$

Applying Property 1 to (6.9),

$$d_n = \frac{m_n + m_{n+1}}{2} \tag{6.10}$$

No matter which approximate solution we choose for d_n, the decision rule is given by

$$r \underset{n}{\overset{n+1}{\gtrless}} d_n. \tag{6.11}$$

In other words,

$$\text{we decide } \hat{n} \text{ if } d_{\hat{n}-1} < r \leq d_{\hat{n}}. \tag{6.12}$$

6.1.3 Error Analysis

For our decision rule, a decision error occurs only when H_n but we decide $\hat{n} \neq n$. Thus, the probability of error for a specific r is

$$p(\epsilon|r) = \sum_{n\neq\hat{n}} f(H_n|r), \tag{6.13}$$

where $f(H|r)$ is related to $f(r|H_i)$ by the Bayesian rule. The total probability of error is obtained by integrating (6.13) over all possible r.

$$p(\epsilon) = \int p(\epsilon|r) f_r(r) dr \tag{6.14}$$

According to Property 4, only $f(r|H = n-1)$ and $f(r|H = n+1)$ could have outstanding value over the decision region $[d_{n-1}, d_n]$.

$$p(\epsilon) \approx \sum_{n=2}^{\infty} \int_{d_{n-1}}^{d_n} [f(r|H_{n-1})p(H_{n-1}) + f(r|H_{n+1})p(H_{n+1})] dr$$

$$
\begin{aligned}
= & \sum_{n=2}^{\infty} \alpha^{n-1} p(H_{n-1}) [Q(\frac{d_{n-1} - m_{n-1}}{\sigma_{n-1}}) - Q(\frac{d_n - m_{n-1}}{\sigma_{n-1}})] \\
& + \alpha^{n+1} p(H_{n+1}) [Q(\frac{m_{n+1} - d_n}{\sigma_{n+1}}) - Q(\frac{m_{n+1} - d_{n-1}}{\sigma_{n+1}})]
\end{aligned} \tag{6.15}
$$

Note that

$$
\begin{aligned}
& \frac{d_n - m_{n-1}}{\sigma_{n-1}} - \frac{d_{n-1} - m_{n-1}}{\sigma_{n-1}} \\
\approx & \frac{d_n - d_{n-1}}{\sigma_{n-1}} \gg 1,
\end{aligned} \tag{6.16}
$$

therefore, $Q(\frac{d_n - m_{n-1}}{\sigma_{n-1}})$ is negligible compared to $Q(\frac{d_{n-1} - m_{n-1}}{\sigma_{n-1}})$. Similarly, $Q(\frac{m_{n+1} - d_n}{\sigma_{n+1}})$ is negligible. (6.15) is approximated by

$$
\begin{aligned}
p(\epsilon) \approx & \alpha^3 p(H_3) Q(\frac{m_3 - d_2}{\sigma_3}) + \sum_{n=3}^{\infty} [\alpha^{n-1} p(H_{n-1}) Q(\frac{d_{n-1} - m_{n-1}}{\sigma_{n-1}}) \\
& + \alpha^{n+1} p(H_{n+1}) Q(\frac{m_{n+1} - d_n}{\sigma_{n+1}})] \\
= & \alpha^2 p(H_2) Q(\frac{d_2 - m_2}{\sigma_2}) + \sum_{n=3}^{\infty} \alpha^n p(H_n) [Q(\frac{m_n - d_{n-1}}{\sigma_n}) \\
& + Q(\frac{d_n - m_n}{\sigma_n})].
\end{aligned} \tag{6.17}
$$

Substituting an appropriate solution of d_n into (6.17) would give us the probability of error within required accuracy. For example, if we choose (6.10),

$$
\begin{aligned}
p(\epsilon) \approx & \alpha^2 p(H_2) Q(\frac{m_3 - m_2}{2\sigma_2}) + \sum_{n=3}^{\infty} \alpha^n p(H_n) [Q(\frac{m_n - m_{n-1}}{2\sigma_n}) \\
& + Q(\frac{m_{n+1} - m_n}{2\sigma_n})].
\end{aligned} \tag{6.18}
$$

6.2 Application Examples

We provide two application examples, latency and energy estimation, in this section. To emphasize the role of the number of hops in the estimation, we use general time and energy models. On how to derive the parameters such as $T_{rx}, T_{tx}$for a specific routing scheme, readers are referred to [105, 111].

6.2.1 Latency Estimation

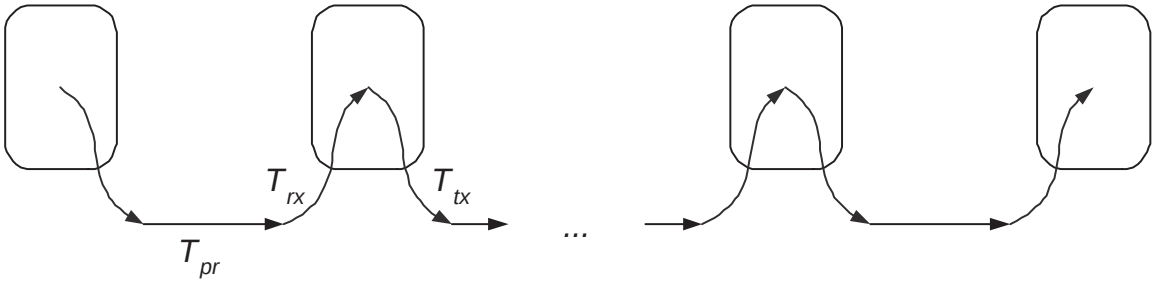

Figure 6.3. Time model.

We use a simple time model, in which the latency increases linearly with the number of hops [112]. Suppose it takes T_{rx}, T_{tx} for a sensor node to process 1 bit of incoming and outgoing message, respectively. And T_{pr} is the required time to transmit 1 bit of message through a band-limited channel. Therefore, the latency introduced for each hop is

$$T_{hop} = T_{tx} + T_{pr} + T_{rx} \tag{6.19}$$

Shown in Fig. 6.3, given the end-to-end distance r, we can find the required number of hops $\hat{n}$ according to (6.11), thus, a good estimator of the total latency of a l-bit message is

$$l\hat{n}T_{hop} \tag{6.20}$$

6.2.2 Energy Consumption Estimation

The following model is adopted from [35] where perfect power control is assumed. To transmit l bits over distance r, the sender's radio expends

$$E_{tx}(l,r) = \begin{cases} lE_{elec} + l\epsilon_{fs}r^2, & r < r_0, \\ lE_{elec} + l\epsilon_{mp}r^4, & r \geq r_0, \end{cases} \tag{6.21}$$

and the receiver's radio expends

$$E_{rx}(l,r) = lE_{elec}. \tag{6.22}$$

E_{elec} is the unit energy consumed by the electronics to process one bit of message, ϵ_{fs} and ϵ_{mp} are the amplifier factor for free-space and multi-path models, respectively, and d_0 is the reference distance to determine which model to use. The values of these communication energy parameters are set as in Table 2.1.

Let s_n denote the single-hop distance from the $(n-1)$th-hop to the nth-hop. Obviously, $s_n \leq R$. In our experimental setting, $R = 30m < d_0$ so that the free space model is always used. This agrees well with most applications, in which multi-hop short-range transmission is preferred to avoid the exponential increase in energy consumption for long-range transmission. Naturally, the end-to-end energy consumption for sending l bits over distance r is given by

$$E_{total}(l, r) = \sum_{1}^{\hat{n}} \{E_{tx}(l, r_1) + E_{rx}(l)\} \tag{6.23}$$

where $\hat{n}$ is the estimated number of hops for given r and r_1 is the single-hop distance because the message is relayed hop by hop.

On the average,

$$\begin{aligned} \bar{E}_{total}(l, r) &= \hat{n}l(E_{elec} + \epsilon_{fs}E[r_1^2] + E_{elec}) \\ &= \hat{n}l(2E_{elec} + \epsilon_{fs}(m_1^2 + \sigma_1^2)) \end{aligned} \tag{6.24}$$

6.2.3 Simulation

We used the same scenario described in Section 6.1.1 and varied the node density λ and transmission range R. In each simulation, the number of hops is estimated for each node using (6.9) and (6.11), and then the latency and energy consumption are estimated using (6.20) and (6.24), respectively. As comparison to our proposed statistic-based estimator, we chose a widely used linear estimator.

$$\begin{aligned} &\text{Linear Estimator 1} \quad \hat{n} = [r/R] + 1, \\ &\text{Linear Estimator 2} \quad \hat{n} = [r/R] + 2, \end{aligned} \tag{6.25}$$

where r is the given distance, R the transmission range and $[r/R]$ is the maximum number less than r/R. We ran extensive simulation for different setting of (N, R_{Bound}, R), but

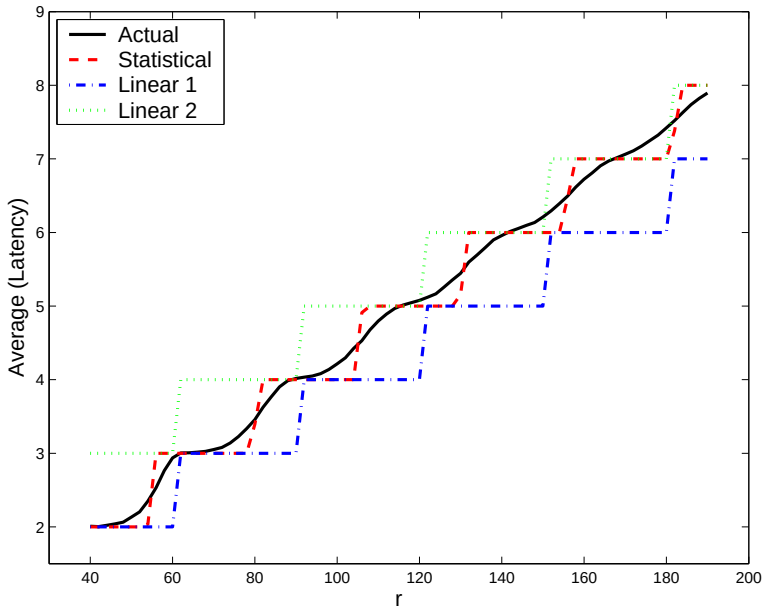

(a)

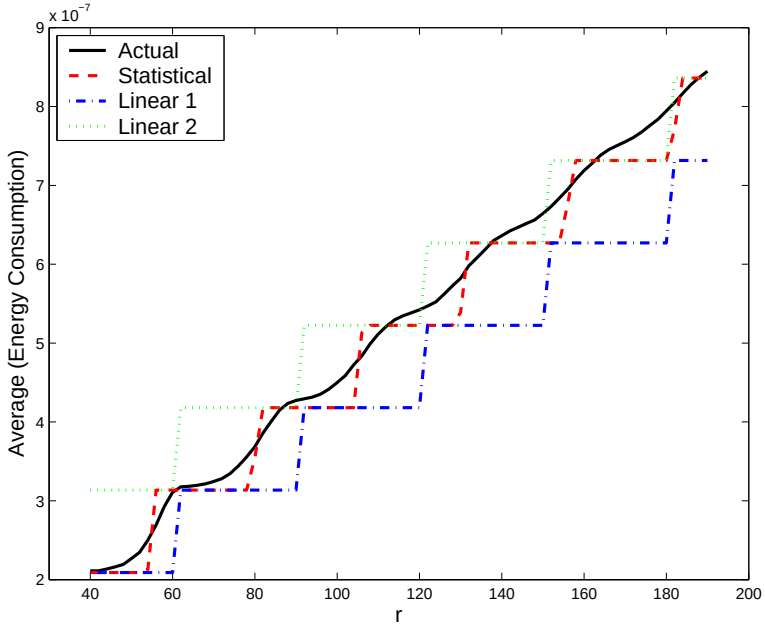

(b)

Figure 6.4. Estimation Average. (a) Latency. (b) Energy consumption.

due to the limit of space, we only plot the results for ($N = 1000, R_{Bound} = 200, R = 30$). The average of latency and energy consumption is shown in Fig.6.4(a) (b) and the RMSE in Fig.6.5(a) (b), respectively. The latency is plotted in units of T_{hop} while the energy consumption in units of Joules. When the distance is less than the transmission range, we can safe decide the number of hops is 1, thus, the estimation error starts

from the transmission range. In addition, the accuracy is not so The ripple shape of RMSE is due to the fact decision errors occurs more often in the overlapping zones of neighboring $f(r|H_i)$. Fig.6.4 show that the linear estimator 1 performs well at the shorter range but suffers visibly at larger range, while the linear estimator does the opposite. The linear estimators, no matter what value their parameters take, may significantly underestimate or overestimate the latency and energy consumption as already pointed out in Section 6.1.1, while our statistic-based model keeps close to the actual latency and energy consumption at all ranges except for the border. This is also verified by Fig.6.5, therefore, the overall RMSE of our estimator is less than 60% of that of linear ones for both latency and energy consumption. These results show that linear models cannot identify network behavior accurately, as also confirmed by our extensive simulations for different settings of node density and transmission range, which is not shown here due to space constraints.

Table 6.2. Estimation RMSE.

	Statistical	Linear 1	Linear 2
Latency	0.4405	0.7489	0.6152
Energy Consumption	4.6584e-008	8.7163e-008	6.1583e-008

6.3 Conclusion

To address the fundamental problem "how many hops does it take for a packet to be relayed for a given distance?", we make both probabilistic and statistic studies. We proposed a Bayesian decision based on the conditional pdf of $f(r|H_i)$. Since $f(r|H_i)$ is computationally complex, we also proposed an attenuated Gaussian approximation for the conditional pdf, which visibly simplifies the decision process and the error analysis. We also show that several linear models, though intuitively sound and widely used, may give significant bias error. We apply our approximation to the latency and energy

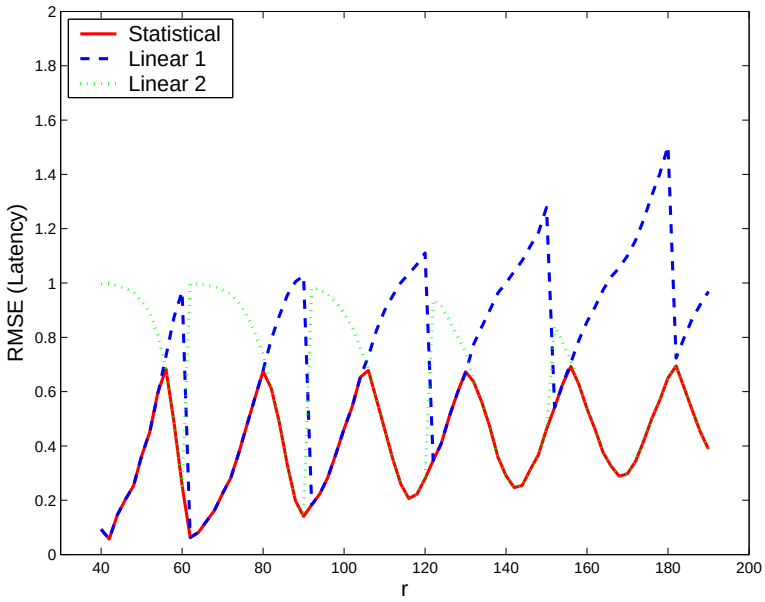

(a)

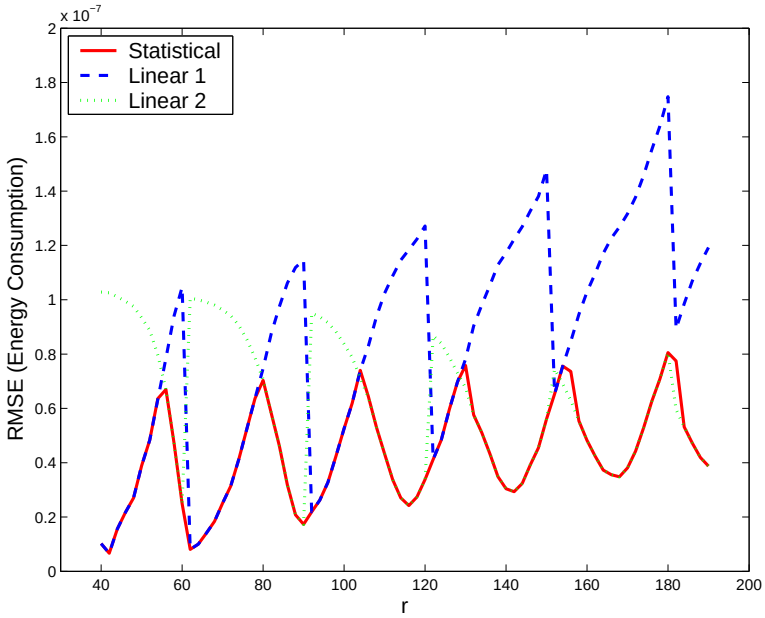

(b)

Figure 6.5. Estimation RMSE. (a) Latency. (b) Energy consumption.

consumption estimation in dense WSN. Simulations show that our approximation model can predict the latency and energy consumption with less than half RMSE, compared to the aforementioned linear models.

CHAPTER 7

CONCLUSION

The previous clustering researches often take a global approach, which is appropriate for global optimization. However, when a distributed clustering is desired, the already-answered questions such as "How many clusters should the nodes be partitioned into?" have to be translated into a distributed version, that is, ''What's the appropriate cluster size?", because it is easier for a node to know its cluster size than the number of clusters in the whole network. In this paper, we take a fully distributed approach to energy efficiency for WSN. Motivated by the local energy efficiency criterion, we propose using the cluster size instead of the number of clusters as the clustering objective parameter in clustering. Furthermore, we utilize the medium contention to implement the headship auction to keep the cluster size within an ideal range. As shown by the simulations, although the proposed MCCHA uses only local information, it achieves better energy efficiency than native LEACH in terms of Data/Energy Ratio and effective lifetime. The simulations also show that the optimal cluster radius obtained from the experiments agrees well with the analysis of optimal clustering, which indicates the performance of our distributed clustering is close to that of the global optimal one.

The clustering research also leads us into modeling of the end-to-end distance for given number of hops in WSN. The experiments showed that the distance does not increase linearly with the number of hops. Therefore, the distance should be analyzed for each number of hops. We derived the distribution for single-hop distance and also showed that the complexity of derivation for multiple-hop distance is beyond practical interest. Thus, we postulate Beta distribution for two-hop end-to-end distance and Gaussian distribution for three-and-more-hop end-to-end distance. Computer simulations showed our

postulated distributions agree well with the histograms. We also show that the distance error can be minimized by exploiting the distribution knowledge.

Furthermore, to address the fundamental problem "how many hops does it take for a packet to be relayed for a given distance?", we make both probabilistic and statistic studies. We proposed a Bayesian decision based on the conditional pdf of $f(r|H_i)$. Since $f(r|H_i)$ is computationally complex, we also proposed an attenuated Gaussian approximation for the conditional pdf, which visibly simplifies the decision process and the error analysis. We also show that several linear models, though intuitively sound and widely used, may give significant bias error. We apply our approximation to the latency and energy consumption estimation in dense WSN. Simulations show that our approximation model can predict the latency and energy consumption with less than half RMSE, compared to the aforementioned linear models.

Although clustering has been well studied for the terrestrial WSN, the unique characteristics of the underwater acoustic communications call for a new study. Because the path loss is not only relevant to the distance, but also related to the working frequency, the optimal cluster size for UW-ASN shows different properties from the terrestrial WSN. In addition, the data aggregation also play an important role in determining the optimal cluster size. The simulation results agrees well with our numerical analysis.

REFERENCES

[1] I. F. Akyildiz, W. Su, Y. Sankarasubramaniam, and E. Cayirci, "A survey on sensor networks," *IEEE Commun. Mag.*, vol. 20, pp. 102–114, Aug. 2002.

[2] A. Ephremides, "Energy concerns in wireless networks," *IEEE Wireless Communications*, vol. 9, no. 4, pp. 48 – 59, Aug 2002.

[3] V. Raghunathan, C. Schurgers, S. Park, and M. Srivastava, "Energy-aware wireless microsensor networks," *IEEE Signal Processing Magazine*, vol. 19, no. 2, pp. 40 – 50, March 2002.

[4] A. Safwati, H. Hassanein, and H. Mouftah, "Optimal cross-layer designs for energy-efficient wireless ad hoc and sensor networks," in *Conference Proceedings of the 2003 IEEE International on Performance, Computing, and Communications Conference 2003*, April 2003, pp. 123 – 128.

[5] Y. Zou and K. Chakrabarty, "Energy-aware target localization in wireless sensor networks," in *Proceedings of the First IEEE International Conference on Pervasive Computing and Communications, 2003. (PerCom 2003)*, March 2003, pp. 60–67.

[6] K. Sohrabi, J. Gao, V. Ailawadhi, and G. J. Pottie, "Protocols for self-organization of a wireless sensor network," *IEEE Personal Commun. Mag.*, vol. 5, no. 7, pp. 16–27, Oct. 2000.

[7] M. Singh and V. Prasanna, "Optimal energy-balanced algorithm for selection in a single hop sensor network," in *Sensor Network Protocols and Applications, 2003. Proceedings of the First IEEE. 2003 IEEE International Workshop on*, 2003, pp. 9–18.

[8] S. Guru, S. Halgamuge, and S. Fernando, "Particle swarm optimisers for cluster formation in wireless sensor networks," in *Intelligent Sensors, Sensor Networks and Information Processing Conference, 2005. Proceedings of the 2005 International Conference on*, 2005, pp. 319–324.

[9] L. Zhao and Q. Liang, "Distributed and energy efficient self-organization for on-off wireless sensor networks," in *15th IEEE Int. Symp. On Personal, Indoor and Mobile Radio Communications (PIMRC'04)*, Barcelona, Spain, September 2004.

[10] ——, "Distributed and energy efficient self-organization for on-off wireless sensor networks," *Int'l Journal of Wireless Information Networks*, vol. 12, pp. 3–9, 2005.

[11] R. Min, M. Bhardwaj, S.-H. Cho, N. Ickes, E. Shih, A. Sinha, A. Wang, and A. Chandrakasan, "Energy-centric enabling technologies for wireless sensor networks," *IEEE Wireless Communications*, vol. 9, no. 4, pp. 28 – 39, Aug. 2002.

[12] T. Shepard, "A channel access scheme for large dense packet radio networks," in *Proc. ACM SIGCOMM*, Stanford, CA, Aug. 1996, pp. 219–230.

[13] M. Ettus, "System capacity, latency and power consumption in multihop-routed ss-cdma wireless networks," in *Proc. Radio and Wireless Conf. (RAWCON'98)*, Colorado Springs, CO, Aug. 1998, pp. 55–58.

[14] B. Das and V. Bharghavan, "Routing in ad-hoc networks using minimum connected dominating sets," in *Proc. IEEE Int. Conf. Communications*, Montreal, QC, Canada, June 1997, pp. 376–380.

[15] B. Das, R. Sivakumar, and V. Bharghavan, "Routing in ad hoc networks using a spine," in *Proc. IEEE Computer Communications and Networks*, Sept. 1997, pp. 34–39.

[16] D. Petrovic, R. Shah, K. Ramchandran, and J. Rabaey, "Data funneling: routing with aggregation and compression for wireless sensor networks," in *Proc. of the First IEEE. Int'l Workshop on Sensor Network Protocols and Applications 2003*, May 2003, pp. 156 –162.

[17] D. J. Baker and A. Ephremides, "The architectural organization of a mobile radio network via a distributed algorithm," vol. COM-29, pp. 1964–1971, Nov. 1981.

[18] D. J. Baker, J. Wieselthier, and A. Ephremides, "A distributed algorithm for scheduling the activation of links in a self-organizing, mobile, radio networks," in *Proc. IEEE Int. Conf. Communications*, June 1982, pp. 2F.6.1–2F.6.4.

[19] D. J. Baker, "Distributed control of broadcast radio networks with changing topologies," in *Proc. IEEE Infocom*, San Diego, CA, Apr. 1983, pp. 49–55.

[20] R. Ramanathan and M. Steenstrup, "Hierarchically-organized, multihop mobile wireless networks for quality-of-service support," *Mobile Networks Appl.*, vol. 3, no. 1, pp. 101–119, 1998.

[21] A. B. McDonald and T. F. Znati, "A mobility-based framework for adaptive clustering in wireless ad hoc networks," *IEEE J. Select. Areas Commun.*, vol. 17, pp. 1466–1487, Aug. 1999.

[22] P. Krishna, N. H. Vaidya, M. Chatterjee, and D. K. Pradhan, "A cluster-based approach for routing in dynamic networks," *ACM Comput. Commun. Rev.*, vol. 17, no. 2, pp. 49 – 64, Apr. 1997.

[23] T. S. Rappaport, *Wireless Communications:Principles and Practice*. Upper Saddle River, NJ: Prentice-Hall, 2002.

[24] M. Gerla and J. T.-C. Tsai, "Multicluster, mobile, multimedia radio network," *ACM J. Wireless Networks*, vol. 1, no. 3, pp. 255–265, 1995.

[25] S. Guru, A. Hsu, S. Halgamuge, and S. Fernando, "Clustering sensor networks using growing self-organising map," in *Intelligent Sensors, Sensor Networks and Information Processing Conference, 2004. Proceedings of the 2004*, 2004, pp. 91–96.

[26] A. J. Haas and B. Liang, "Ad hoc mobility management with uniform quorum systems," *IEEE/ACM Trans. Networking*, vol. 7, pp. 228–240, Apr. 1999.

[27] T.-C. Hou and T.-J. Tsai, "An access-based clustering protocol for multihop wireless ad hoc networks," *IEEE J. Select. Areas Commun.*, vol. 19, pp. 1201–1210, July 2001.

[28] A. Iwata, C.-C. Chiang, G. Pei, M. Gerla, and T.-W. Chen, "Scalable routing strategies for ad hoc wireless networks," *IEEE J. Select. Areas Commun.*, vol. 17, pp. 1369–1679, Aug. 1999.

[29] C. R. Lin and M. Gerla, "A distributed control scheme in multi-hop packet radio networks for voice/data traffic support," in *Proc. IEEE Int. conf. Communications*, Seattle, WA, June 1995, pp. 1238–1242.

[30] ——, "Adaptive clustering for mobile wireless networks," *IEEE J. Select. Areas Commun.*, vol. 15, pp. 1265–1275, Sept. 1997.

[31] J.-S. Liu and C.-H. Lin, "Power-efficiency clustering method with power-limit constraint for sensor networks," in *Proc. of the 2003 IEEE International Conference on Performance, Computing, and Communications*, Apr 2003, pp. 129 –136.

[32] C.-M. Liu and C.-H. Lee, "Power efficient communication protocols for data gathering on mobile sensor networks," in *Vehicular Technology Conference, 2004. VTC2004-Fall. 2004 IEEE 60th*, vol. 7, 2004, pp. 4635–4639 Vol. 7.

[33] M. Dhanaraj, B. Manoj, and C. Murthy, "A new energy efficient protocol for minimizing multi-hop latency in wireless sensor networks," in *Pervasive Computing and Communications, 2005. PerCom 2005. Third IEEE International Conference on*, 2005, pp. 117–126.

[34] M. Younis, M. Bangad, and K. Akkaya, "Base-station repositioning for optimized performance of sensor networks," in *Vehicular Technology Conference, 2003. VTC 2003-Fall. 2003 IEEE 58th*, vol. 5, 2003, pp. 2956–2960 Vol.5.

[35] W. B. Heinzelman, A. P. Chandrakasan, and H. Balakrishnan, "An application-specific protocol architecture for wireless microsensor networks," *IEEE Trans. Wireless Commun.*, vol. 1, no. 4, pp. 660 – 670, Oct. 2002.

[36] V. Mhatre and C. Rosenberg, "Homogeneous vs heterogeneous clustered sensor networks: a comparative study," in *2004 IEEE International Conference on Communications*, vol. 6, 2004, pp. 3646–3651 Vol.6.

[37] M. Younis, K. Akkaya, and A. Kunjithapatham, "Optimization of task allocation in a cluster-based sensor network," in *Computers and Communication, 2003. (ISCC 2003). Proceedings. Eighth IEEE International Symposium on*, 2003, pp. 329–334 vol.1.

[38] O. Younis and S. Fahmy, "Heed: a hybrid, energy-efficient, distributed clustering approach for ad hoc sensor networks," *Mobile Computing, IEEE Transactions on*, vol. 3, no. 4, pp. 366–379, 2004.

[39] G. Xing, C. Lu, R. Pless, and Q. Huang, "Impact of sensing coverage on greedy geographic routing algorithms," *Parallel and Distributed Systems, IEEE Transactions on*, vol. 17, no. 4, pp. 348–360, 2006.

[40] H. Frey, "Scalable geographic routing algorithms for wireless ad hoc networks," *Network, IEEE*, vol. 18, no. 4, pp. 18–22, 2004.

[41] J. Hightower and G. Borriello, "Location systems for ubiquitous computing," *IEEE Computer*, vol. 34, no. 8, pp. 57–66, August 2001.

[42] N. Bulusu, J. Heidemann, D. Estrin, and T. Tran, "Self-configuring localization systems: Design and experimental evaluation," *ACM Transactions on Embedded Computing Systems (TECS)*, vol. 3, pp. 24 – 60, February 2004. [Online]. Available: http://portal.acm.org/citation.cfm?id=972630

[43] S. Caruso, A and; Chessa, S. De, and A. Urpi, "Gps free coordinate assignment and routing in wireless sensor networks," in *IEEE Infocom*, March 2005.

[44] A. Savvides and M. B. Strivastava, "Distributed fine-grained localization in ad-hoc networks," *IEEE Transactions on Mobile Computing*, 2003.

[45] K. Seada, A. Helmy, and R. Govindan, "On the effect of localization errors on geographic face routing in sensor networks," in *Information Processing in Sensor Networks, 2004. IPSN 2004. Third International Symposium on*, 2004, pp. 71–80.

[46] C. E. Dadson, J. Durkin, and E. Martin, "Computer prediction of field strength in the planning of radio systems," *IEEE Trans. Veh. Technol.*, vol. VT-24, no. 1, pp. 1–7, Feb 1975.

[47] R. Edwards and J. Durkin, "Computer prediction of service area for vhf mobile radio networks," in *Proceedings of the IEE*, vol. 116, no. 9, 1969, pp. 1493–1500.

[48] A. G. Longley and P. L. Rice, "Prediction of tropospheric radio transmission loss over irregular terrain; a computer method," *ESSA Technical Report*, 1968.

[49] T. Okumur, E. Ohmori, and K. Fukuda, "Field strength and its variability in vhf and uhf land mobile service," *Review Electrical Communication Laboratory*, vol. 16, no. 9-10, pp. 825–873, Sept-Oct 1968.

[50] P. L. Rice, A. G. Longley, K. A. Norton, and A. Barsis, "Transmission loss predictions for tropospheric communication circuits," *NBS Tech Note 101*, 1967.

[51] J. Walfisch and H. L. Bertoni, "A theoretical model of uhf propagation in urban environments," *IEEE Trans. Antennas Propagat.*, vol. AP-36, pp. 1788–1796, October 1988.

[52] E. Elnahrawy, X. Li, and R. Martin, "The limits of localization using signal strength: a comparative study," in *Sensor and Ad Hoc Communications and Networks, 2004. IEEE SECON 2004. 2004 First Annual IEEE Communications Society Conference on*, 2004, pp. 406–414.

[53] D. Niculescu and B. Nath, "Ad hoc positioning system (aps)," in *Global Telecommunications Conference, 2001. GLOBECOM '01. IEEE*, vol. 5, 2001, pp. 2926–2931 vol.5.

[54] ——, "Dv based positioning in ad hoc networks," *Telecommunication Systems*, vol. 22(1-4), pp. 267–280, 2003.

[55] C. Savarese, J. Rabay, and K. Langendoen, "Robust positioning algorithms for distributed ad-hoc wireless sensor networks," in *USENIX Technical Annual Conference*, Monterey, CA, June 2002.

[56] I. F. Akyildiz, D. Pompili, and T. Melodia, "Challenges for efficient communication in underwater acoustic sensor networks," *IEEE ACM Sigbed Review*, vol. 1, no. 2, July 2004.

[57] A. Mussa, W. Sandham, and T. Durrani, "Underwater robotics navigation using multi-sensor fusion," in *Underwater Applications of Image Processing (Ref. No. 1998/217), IEE Colloquium on*, 1998, pp. 5/1–5/9.

[58] L. Antonelli and F. Blackmon, "Experimental investigation of optical, remote, aerial sonar," in *Oceans '02 MTS/IEEE*, vol. 4, 2002, pp. 1949–1955 vol.4.

[59] I. F. Akyildiz, D. Pompili, and T. Melodia, "Underwater acoustic sensor networks: Research challenges," *Ad Hoc Networks (Elsevier)*, vol. 3, no. 3, pp. 257–279, May 2005.

[60] P. C. Etter, "Recent Advances in Underwater Acoustic Modelling and Simulation," *Journal of Sound Vibration*, vol. 240, pp. 351–383, Feb. 2001.

[61] K. Nasahashi, T. Ura, A. Asada, T. Obara, T. Sakamaki, K. Kim, and K. Okamura, "Underwater volcano observation by autonomous underwater vehicle "r2d4"," in *Oceans 2005 - Europe*, vol. 1, 2005, pp. 557–562 Vol. 1.

[62] M. Ishii, S. Oshiro, and T. Itoh, "The development and utilization of the “underwaterbackhoe,” a multifunctional underwater construction machine," in *Underwater Technology, 2000. UT 00. Proceedings of the 2000 International Symposium on*, 2000, pp. 319–322.

[63] G. Rajasegaran, G. Taha, and S. Ramachandran, "Design and development of an underwater vehicle with the structure mounted on spheres," in *Control, Automation, Robotics and Vision, 2002. ICARCV 2002. 7th International Conference on*, vol. 3, 2002, pp. 1470–1474 vol.3.

[64] M. Stojanovic, "Recent advances in high-speed underwater acoustic communications," *Oceanic Engineering, IEEE Journal of*, vol. 21, no. 2, pp. 125–136, 1996.

[65] D. Kilfoyle and A. Baggeroer, "The state of the art in underwater acoustic telemetry," *Oceanic Engineering, IEEE Journal of*, vol. 25, no. 1, pp. 4–27, 2000.

[66] J.-K. Yeo, Y.-K. Lim, and H.-H. Lee, "Modified mac (media access control) protocol design for theacoustic-based underwater digital data communication," in *Industrial Electronics, 2001. Proceedings. ISIE 2001. IEEE International Symposium on*, vol. 1, 2001, pp. 364–368 vol.1.

[67] J. Catipovic, "Performance limitations in underwater acoustic tlemetry," *IEEE Journal of Oceanic Engineering*, vol. 15, pp. 205–216, July 1990.

[68] S. Shahabudeen and M. Chitre, "Design of networking protocols for shallow water peer-to-peer acoustic networks," in *Oceans 2005 - Europe*, vol. 1, 2005, pp. 628–633 Vol. 1.

[69] R. Urick, *Principles of Underwater Sound*. Mcgraw-Hill, 1983.

[70] *Wireless LAN Medium Access Control(MAC) and Physical Layer(PHY) Specifications*, 1997.

[71] L. Bao and J. Garcia-Luna-Aceves, "Hybrid channel access scheduling in ad hoc networks," in *Proc. IEEE Tenth Int'l Conf on Network Protocols (ICNP)*, November 2002.

[72] W. Rajendran, K. Obraczka, and J. Garcia-Luna-Aceves, "Energy-efficient, collision-free medium access control for wireless sensor networks," in *Proc. First Int'l Conf on Embedded Networked Sensor Systems*, November 2003.

[73] S. Pradhan, J. Kusuma, and K. Ramchandran, "Distributed compression in a dense microsensor network," *IEEE Signal Processing Mag.*, vol. 19, no. 2, pp. 51–60, Mar 2002.

[74] A. Boulis, S. Ganeriwal, and M. Srivastava, "Aggregation in sensor networks: an energy-accuracy trade-off," in *Proceedings of the First IEEE International Workshop on Sensor Network Protocols and Applications*, May 2003, pp. 128–138.

[75] W. Chen, N. Jain, and S. Singh, "Anmp:ad hoc network management protocol," *IEEE J. Select. Areas Commun.*, vol. 17, pp. 1506–1531, Aug. 1999.

[76] J. Manyika and H. Durrrant-Whyte, *Data Fusion and Sensor Management: A Decentralized Information-Theoretic Approach*. Ellis Horwood Limited, 1994.

[77] A. J. Viterbi, *CDMA:principles of spread spectrum communication*. Reading, MA: Addison-Wesley, 1995.

[78] C. F. Chiasserinia and R. R. Rao, "Pulsed battery discharge in communication devices," in *Proc. Mobicom*, 1999, pp. 88–95.

[79] T.-C. Hou and V. Li, "Transmission range control in multihop packet radio networks," *IEEE Transactions on Communications*, vol. 34, no. 1, pp. 38–44, 1986.

[80] Y.-C. Cheng and T. Robertazzi, "Critical connectivity phenomena in multihop radio models," *IEEE Transactions on Communications*, vol. 37, no. 7, pp. 770–777, 1989.

[81] S. Vural and E. Ekici, "Analysis of hop-distance relationship in spatially random sensor networks," in *MobiHoc '05: Proceedings of the 6th ACM international symposium on Mobile ad hoc networking and computing*. New York, NY, USA: ACM Press, 2005, pp. 320–331.

[82] M. Zorzi and R. Rao, "Geographic random forwarding (geraf) for ad hoc and sensor networks: multihop performance," *Mobile Computing, IEEE Transactions on*, vol. 2, no. 4, pp. 337–348, 2003.

[83] S. Chandler, "Calculation of number of relay hops required in randomly located radio network," *Electronics Letters*, vol. 25, no. 24, pp. 1669–1671, 1989.

[84] S. Mukherjee and D. Avidor, "On the probability distribution of the minimal number of hops between any pair of nodes in a bounded wireless ad-hoc network subject to fading," in *Proceedings of the 2nd International Workshop on Wireless Ad-Hoc Networks*, Kings College, London, UK, May 2005.

[85] G. Snedecor and W. Cochran, *Statistical Methods*. Iowa State University Press / AMES, 1989.

[86] R. Jurdak, C. V. Lopes, and P. Baldi, "Battery lifetime estimation and optimization for underwater sensor networks," in *IEEE Sensor Network Operations*. IEEE Press, Winter 2004.

[87] F. Fisher and V. Simmons, "Sound absorption in sea water," *Journal of Acoustical Society of America*, vol. 62, p. 558, 1977.

[88] J. C. Bezdek, *Pattern recognition with fuzzy objective function algorithms*. New York: Plenum Press, 1981.

[89] R. Jurdak, C. V. Lopes, and P. Baldiy, "A framework for modeling sensor networks," in *Proc. Workshop on Building Software for Pervasive Computing(OOPSLA'04)*, Oct 2004.

[90] Q. Liang, "A design methodology for wireless personal area networks with power efficiency," in *IEEE Wireless Communications and Networking 2003(WCNC'03)*, vol. 3, 2003, pp. 16–20.

[91] L. Zhao, X. Hong, and Q. Liang, "Energy-efficient self-organization for wireless sensor networks: A fully distributed approach," in *IEEE Globecom'04*. Dallas, TX: IEEE, Dec 2004.

[92] L. Zhao and Q. Liang, "Optimal cluster size for underwater acoustic networks," *submitted to IEEE Journal of Oceanic Engineering*.

[93] C. C. Chang, C. Y. Chang, and Y. T. Cheng, "Distance measurement technology development at remotely teleoperated robotic manipulator system for underwater constructions," in *Underwater Technology, 2004. UT '04. 2004 International Symposium on*, 2004, pp. 333–338.

[94] K. Shirai, J. Akizono, and T. Hirabayashi, "Development of underwater ultrasonic positioning system for construction machines," in *Underwater Technology, 2004. UT '04. 2004 International Symposium on*, 2004, pp. 139–144.

[95] "Underwater acoustic modem." available:www.link-quest.com.

[96] L. Zhao and Q. Liang, "Optimal cluster size for underwater acoustic networks," in *submitted to Int'l Workshop on Wireless Ad-hoc Networks (IWWAN'06)*, 2006.

[97] ——, "Resource allocation and latency estimation in sensor networks using maximum likelihood decision," *submitted to IEEE Trans. Computer*.

[98] L. Fang, W. Du, and P. Ning, "A beacon-less location discovery scheme for wireless sensor networks," in *IEEE Infocom*, March 2005.

[99] Q. Huang, C. Lu, and G.-C. Roman, "Spatiotemporal multicast in sensor networks," in *SenSys '03: Proceedings of the 1st international conference on Embedded networked sensor systems*. New York, NY, USA: ACM Press, 2003, pp. 205–217.

[100] H. Lim and J. Hou, "Localization for anisotropic sensor networks," in *IEEE Infocom'05*, March 2005.

[101] N. Priyantha, H. Balakrishnan, E. Demaine, and S. Teller, "Mobile-assisted localization in wireless sensor networks," in *IEEE Infocom*, March 2005.

[102] L. Zhao and Q. Liang, "Fuzzy deployment for wireless sensor networks," in *IEEE Int'l Conference on Computational Intelligence for Homeland Security and Personal Safety*, Orlando, FL, March 2005.

[103] R. Jain, A. Puri, and R. Sengupta, "Geographical routing using partial information for wireless ad hoc networks," *IEEE Personal Communications*, vol. 8, pp. 48 – 57, Feb 2001.

[104] Y. Xu, J. Heidemann, and D. Estrin, "Geography-informed energy conservation for ad hoc routing," in *MobiCom '01: Proceedings of the 7th annual international conference on Mobile computing and networking*. New York, NY, USA: ACM Press, 2001, pp. 70–84.

[105] M. Zorzi and R. Rao, "Geographic random forwarding (geraf) for ad hoc and sensor networks: energy and latency performance," *IEEE Transactions on Mobile Computing*, vol. 2, no. 4, pp. 349–365, 2003.

[106] P. Y. Xu and Z. L. Jun, "Virtual destination based geographic routing in ad hoc mobile networks," in *Wireless Communications, Networking and Mobile Computing, 2005. Proceedings. 2005 International Conference on*, vol. 2, 2005.

[107] D. Son, A. Helmy, and B. Krishnamachari, "The effect of mobility-induced location errors on geographic routing in ad hoc networks: analysis and improvement using mobility prediction," in *Wireless Communications and Networking Conference, 2004. WCNC. 2004 IEEE*, vol. 1, 2004.

[108] S. Das, H. Pucha, and Y. Hu, "Performance comparison of scalable location services for geographic ad hoc routing," in *INFOCOM 2005. 24th Annual Joint Conference of the IEEE Computer and Communications Societies. Proceedings IEEE*, vol. 2, 2005.

[109] M. G. Kendall and P. A. P. Moran, *Geometrical Probability*. Charles Griffin & Co. Ltd., 1963.

[110] L. Zhao and Q. Liang, "Modeling end-to-end distance for given number of hops in wireless sensor networks," in *submitted to Globecom"06*, 2006.

[111] H. M. Ammari and S. K. Das, "Trade-off between energy savings and source-to-sink delay in data dissemination for wireless sensor networks," in *MSWiM '05: Proceedings of the 8th ACM international symposium on Modeling, analysis and simulation of wireless and mobile systems.* New York, NY, USA: ACM Press, 2005, pp. 126–133.

[112] W. Ye, J. Heidemann, and D. Estrin, "Medium access control with coordinated adaptive sleeping for wireless sensor networks," *IEEE/ACM Trans. Networking*, vol. 12, no. 3, pp. 493–506, 2004.

BIOGRAPHICAL STATEMENT

Liang Zhao received his B.S. degree and M.S. degrees from University of Science and Technology of China in 1997 and 2000, respectively, both in Electrical Engineering. From 2000 to 2001, he was with Huawei Technologies as a Technical Staff Member. His current research interest includes self-organization, scheduling and energy efficiency in wireless sensor networks. He is a student member of IEEE Communications society.